To the Graduate Council:

I am submitting herewith a thesis written by BO CHEN entitled " A Numerical Method for the Incompressible Navier-Stokes Equations with Application to Two-Phase Flow". I have examined the final copy of this thesis for form and content and recommend that it be accepted in partial fulfillment of the requirements for the degree of Master of Science, with a major in Mathematics.

Vasilios Alexiades, Major Professor

We have read this thesis
and recommend its acceptance:

Suzanne Lenhart

Wongkwan

Accepted for the Council:

Interim Vice Provost
and Dean of the Graduate School

A Numerical Method for the Incompressible Navier-Stokes Equations with Application to Two-Phase Flow

A Thesis

Presented for the

Master of Science Degree

The University of Tennessee, Knoxville

Bo Chen

December, 2000

Acknowledgments

I would like to express gratitude to my supervisor, Dr. Vasilios Alexiades for his continuous guidance and encouragement, his endless patience and friendly help

I am very grateful to Dr Kwai L. Wong at Joint Institute for computational Science and Dr. Yong X Tao at Tennessee State University The financial support from NSF grant is highly acknowledged

Many thanks also goes to Dr Christian Halloy, Mrs Mary Drake at Joint Institute for Computational Science, UTK for their help and patience.

I would like to thank my committee member, Dr Suzanne Lenhart at Mathematics department for her critical comments and stimulating questions when reading the first version of this report and in her PDE course

I am also very in-debt to Drs A Jerry Baker, Joe Iannelli and Allen N. Yu at Mechanical and Aerospace Engineering and Engineering Science department Their enlightening instructions and help during my study in the department will be always in my mind.

I also appreciate the help from my colleagues and friends

Special thanks goes to Dr. Tzusheng Pei at Computer Science department and Mr Mike Saum at Mathematics department. They provided me very detailed help of how to use the LaTeXpackage so that I could prepare this thesis in time

Finally I thank all my family members for their love, understanding, patience and support in the decades of my life.

Abstract

A finite difference numerical method is developed for the simulation of time-dependent incompressible Navier-Stokes equations

As in the original projection method developed by Chorin, we first solve diffusion-convection equations to predict a intermediate velocity field which are then projected onto the space of divergence-free field. We integrate the diffusion-convection by θ implicit scheme and solve the pressure Poisson equation by successive over-relaxation method. The second order centered difference is employed to discretize both the convective and viscous terms

We develop two-dimensional and three-dimensional computer programs in Fortran language Numerical results are presented

We couple our inpressible Navier-Stokes solver with an interacting continuum model for two-phase flows with heat, mass transfer and phase change The Volume of Fluid method is employed in the present study Two example simulations are presented, convective melting of solid particles in a fluid under micro-gravity, and a three dimensional driven cavity problem.

Contents

Chapter 1	Introduction	1
Chapter 2	Equation of Motion	5
Chapter 3	Projection Method	12
Chapter 4	A Numerical Method for the INS	17
Chapter 5	A Continuum Model for Two-Phase Flows	29
Chapter 6	Results and Discussion	37
Reference		54
Vita		57

List of Figures

1 Velocity profile of a developed duct flow 39

2 Velocity vector and streamlines of the driven cavity flow at Re=400 40

3 Velocity vector and streamlines of the driven cavity flow at Re=1000 41

4 Velocity vector and streamlines of the driven cavity flow at Re=3200 41

5 Velocity vector and streamlines of the driven cavity flow at Re=5000 42

6 The tertiary corner eddy in the driven cavity flow at Re=5000 43

7 Temperature contour of the thermo driven cavity flow at Ra=100 46

8 Velocity vector and streamlines of the thermo driven cavity flow at Ra=100 46

9 Velocity vector of a two-phase flow, melting of ice in water . . 48

10 Velocity vector plot of the 3D driven cavity flow at z=0.5 plane . 50

11 Velocity vector plot of the 3D driven cavity flow at y=0.5 plane 51

12 Velocity vector plot of the 3D driven cavity flow at x=0.5 plane 52

Chapter 1
Introduction

The Navier-Stokes equations are the equations governing the motion of usual fluids like water, air, and oil, under quite general conditions They appear in the study of many important phenomena, either alone or coupled with other equations. They are derived under the physical assumption that there exists a linear local relation between stress and strain rates

The Navier-Stokes equations are nonlinear. The nonlinear term contained in the equations comes from kinematical considerations (i.e., it is inherent in the motion) and does not result from assumptions about the physical model Consequently this term can not be avoided by changing the physical model [20] This makes the the mathematical study of these equations difficult, although the physical model leading to the Navier-Stokes equations is quite simple.

The exact solutions of Navier-Stokes equations are very difficult to reach In fact, we know just a few exact solutions, almost all of which are obtained under some significant simplifications of domain and the equations (i e , the nonlinear terms are removed). Therefore, these solutions are not as helpful to people as expected.

On the other hand, the huge demand of knowledge of fluid field continuously motivates the efforts to search for accurate and efficient numerical solutions of the Navier-Stokes equations So far, a dozen of numerical algorithms have been developed and played an important role in several scientific and engineering fields Thorough review of current status of numerical methods for Navier-Stokes equations can be found in [16] and [23]

Among these methods, one class with solid mathematical foundation is the projection method. The philosophy of projection method is the orthogonal decomposition of a vector-valued function in a Hilbert Space This orthogonality

property is reflected in the Hodge decomposition which states that a vector field can be uniquely decomposed into a divergence-free component $\mathbf{u}^d$ that satisfies $\mathbf{u}^d \quad n = 0$ and the gradient of some scalar ϕ. Furthermore, if we integrate by parts, we obtain that

$$\int_\Omega \mathbf{u}^d \cdot \nabla\phi \, dx = 0. \tag{1}$$

Consequently, the Hodge decomposition defines an orthogonal projection $\mathcal{P}$ on L^2 such that $\mathcal{P}\mathbf{u} = \mathbf{u}^d$. By using this projection, one can interpret the incompressible Navier-Stokes equations as an evolution equation for velocity within the space of divergence-free vector fields [3].

This idea was first applied in [15], [20] to prove the existence and uniqueness of the solution of Navier-Stokes equations. In 1969, Chorin [4] and Temam [20] applied it to numerical methods simultaneously After their original papers, some efforts have been devoted to improve the accuracy and several variants of their original methods have been developed [3], [14], [19], [22]

Chorin's method is based on a discrete form of the Hodge decomposition. In this method, we first comput an intermediate vector field, which is then projected onto divergence-free fields to recover the velocity. The calculation of the discrete Hodge projection involves discretizing the Navier-Stokes equations and using the resulting discrete operator and its adjoint to form the projection

The most widely used discretization methods of Navier-Stokes equations can be fall into three categories finite difference, finite element and finite volume method

The finite difference method is the oldest and simplest one Its idea can be traced back to Euler in the 18th century. This method is based on the Taylor expansion and can be applied to PDEs straightforwardly

The discovery of the finite element method is attributed to some structural

engineers In this method the space domain is discretized into a finite number of small, non-overlapping elements with more arbitrary shape and size Normally the numerical unknowns are stored at the vertices (or nodes) of these elements. In each element the field variables are approximated by linear combinations of local interpolation functions using the nodal values. These small elements can be assembled by a variational principle or weighted residuals method to form an algebraic system In the jargon of structural engineers, these matrices are called stiffness matrix and mass matrix

The most physically intuitive method is the finite volume method, in which the physical space is divided into a finite number of control volumes, or cells, and the integral form of the conservation law is applied directly to these control volumes. This assures that such quantities as mass, momentum and energy conserved at the discrete level. The great advantage of both finite element and finite volume method is their flexibility in dealing with complex geometry

In the present study, we present a numerical method based on Chorin's projection method and finite difference discretization. It is first order accurate in time and second order accurate in space

We restrict our attention to homogeneous boundary conditions. We assume that the mesh spacing is uniform in the x, y and z directions

The presentation is organized in the following order.

In chapter 2, we briefly describe the basic equations of fluid mechanics and derive the incompressible Euler and Navier-Stokes equations and the boundary conditions for well-posedness.

In chapter 3, we present a detailed description of the projection method for the incompressible Navier-Stokes equations.

In chapter 4, we describe the details of our numerical method, including the time-stepping procedure in a semi-discrete form, a spatial discretization for a divergence form nonlinear advection-diffusion equations, the Gauss-Siedel iteration

for the pressure Poisson equation and a discussion of an upwind method for the volume-of-fluid advection equation, which is usually coupled with the incompressible Navier-Stokes equations to calculate the problems with free-boundaries.

In chapter 5, we discuss the implementation details and computational results Five test cases are given with further discussions. At the end of this chapter, we present the numerical results for a benchmark problem, the driven cavity flow in $\mathbf{R}^3$, which reveals some three dimensional spatial structures of the flow

Chapter 2
Equations of Motion

In this chapter, we briefly describe the basic equations of fluid mechanics. These equations are derived from the conservation laws of mass, momentum and energy

§2.1 Euler's equations

We begin with the simplest assumptions, leading to Euler's equations for a perfect fluid.

Let D be a region in two- or three-dimensional space R^d $(d = 2, 3)$, filled with a fluid Let $\mathbf{x} \in D$ be a point in D and consider the the particle of fluid moving through $\mathbf{x}$ at time t. The dependent variables in the *Eulerian* description of fluid mechanics are the fluid density $\rho(\mathbf{x}, t)$, the velocity vector field $\mathbf{u}(\mathbf{x}, t)$, and the pressure field $p(\mathbf{x}, t)$ We temporarily assume that the quantities are smooth enough so that the standard operations of calculus can be performed on them.

The fundamental kinematic principle is expressed by the notion of the *convective derivative.* The rate of change of a quantity given by the function $f(\mathbf{x}, t)$ along a flow line is

$$\begin{aligned} \frac{df(\mathbf{x}, t)}{dt} &= \lim_{\delta t \to 0} \frac{f(\mathbf{x} + \mathbf{u}\delta t, t + \delta t) - f(\mathbf{x}, t)}{\delta t} \\ &= \frac{\partial f(\mathbf{x}, t)}{\partial t} + \mathbf{u} \quad \nabla f(\mathbf{x}, t). \end{aligned} \tag{2}$$

The fundamental equations of motion for a fluid system are equations for $\rho(\mathbf{x}, t)$, $\mathbf{u}(\mathbf{x}, t) = (u_1, u_2, u_3)$ and $p(\mathbf{x}, t)$.

Consider the volume δV of an element of mass δm as the system evolves Conservation of mass means that δm does not change for this element If the

element compresses or expands then the volume and density will change, but the mass is fixed

$$\frac{d\delta m}{dt} = 0. \tag{3}$$

The rate of change of the volume occupied by δm is obtained as follows For a rectangular volume $\delta V = \delta x \delta y \delta z$ we write

$$\frac{d\delta V}{dt} = \frac{d\delta x}{dt}\delta y \delta z + \frac{d\delta y}{dt}\delta x \delta z + \frac{d\delta z}{dt}\delta x \delta y \tag{4}$$

The length elements increase or decrease according to the relative velocity of their endpoints. The rate of change of the length δx is

$$\frac{d\delta x}{dt} = u_1(x + \delta x/2, y, z, t) - u_1(x - \delta x/2, y, z, t) = \frac{\partial u_1}{\partial x}\delta x, \tag{5}$$

and likewise for the other components. Combined with equation (4), this gives

$$\frac{d\delta V}{dt} = (\nabla \cdot \mathbf{u})\delta V \tag{6}$$

Hence the divergence of the velocity vector field is the local rate of change of the volume of elements of mass. In terms of the density ρ,

$$\frac{d\rho}{dt} = \frac{d}{dt}\frac{\delta m}{\delta V} = -\frac{\delta m}{(\delta V)^2}\frac{d\delta V}{dt} = -\rho\nabla \quad \mathbf{u} \tag{7}$$

Using the definition of the convective derivative, we see that conservation of mass manifests itself as the *continuity equation*

$$0 = \frac{\partial \rho}{\partial t} + \mathbf{u} \cdot \nabla\rho + \rho\nabla \cdot \mathbf{u} = \frac{\partial \rho}{\partial t} + \nabla \cdot (\rho\mathbf{u}) \tag{8}$$

Newton's second law of motion, which states that the rate of change of momentum equals the net applied force, can be applied to each element of mass in the fluid In the absence of any externally applied forces, the net force δF acting

on each element of mass is due to the pressure field The component of force in the x-direction is

$$\delta F_1 = p(\mathbf{x} - \hat{\mathbf{i}}\delta x/2, t)\delta y \delta z - p(\mathbf{x} + \hat{\mathbf{i}}\delta x/2, t)\delta y \delta z = -\frac{\partial p}{\partial x}\delta V \tag{9}$$

Similar expressions hold for the y and z components of the force Hence Newton's second law for the element of fluid mass δm at position δx is,

$$\frac{d}{dt}(\delta m \mathbf{u}(\mathbf{x}, t)) = \delta F = -\delta V \nabla p. \tag{10}$$

Recalling the equation of conservation of mass (3) and the definition of the convective derivative and dividing through by δm we obtain the *Euler's Equations*

$$\frac{\partial \mathbf{u}}{\partial t} + \mathbf{u} \cdot \nabla \mathbf{u} = -\frac{1}{\rho}\nabla p \tag{11}$$

Combined, the continuity equation and Euler's equations provide $d+1$ evolution equations for the $d+2$ dependent variables (ρ, p and the d components of $\mathbf{u}$). What remains is to provide a connection between density and pressure Typically this is in the form of a thermodynamic equation of state. For example, in an ideal gas at constant temperature, $p \sim \rho$. If temperature variations are to be accounted for, then the pressure may become a function of both the local density and the local temperature and a further evolution equation for the temperature must be supplied. A significant simplification is achieved by considering fluids which are effectively incompressible Mathematically the condition of incompressibility is simply

$$\nabla \quad \mathbf{u} = 0 \tag{12}$$

Physically, this constraint restricts applicability to problems where all the relevant velocities are much less than the speed of sound in the fluid The continuity equation (8) then implies that the convective derivative of the density vanishes,

so the density of each fluid element never changes from its initial value This, in turn, implies that an initially homogeneous (constant density) fluid remains so .

$$\rho(\mathbf{x}, 0) = \text{constant} \qquad \Rightarrow \qquad \rho(\mathbf{x}, t) = \text{constant} \tag{13}$$

Euler's equations for an incompressible homogeneous fluid are

$$\frac{\partial \mathbf{u}}{\partial t} + \mathbf{u} \cdot \nabla \mathbf{u} + \frac{1}{\rho} \nabla p = 0 \tag{14}$$

$$\nabla \cdot \mathbf{u} = 0, \tag{15}$$

where the density is now a parameter These are $d+1$ equations for the $d+1$ unknowns (p and the d components of $\mathbf{u}$).

Boundary conditions are determined by the physics of the problem at hand If the fluid is confined to a fixed region Ω of space bounded by a stationary boundary $\partial\Omega$, then the fluid can not cross these rigid boundaries This means that the normal component of the velocity vector field satisfies

$$\mathbf{n} \cdot \mathbf{u}|_{\partial\Omega} = 0, \tag{16}$$

where $\mathbf{n}$ is the local normal to $\partial\Omega$

§2.2 Incompressible Navier-Stokes equations

Viscosity is the tendency of a fluid to resist shearing motions. As such, it is a frictional force with its origins in the microscopic interactions between the atoms or molecules making up the fluid Its net effect is to dissipate organized, macroscopic forms of energy- the kinetic energy in the flow field - and convert it to the disorganized, microscopic form of energy - heat. Shearing forces in continuum mechanical systems are described by the stress tensor. The tensorial nature of

these forces results from the fact that there are two directions associated with each such force, the direction of the force itself and the orientation of the area across which the force acts.

Consider a rectangular shaped portion of fluid, centered at the point (x, y, z) with side lengths $(\delta x,\ \delta y,\ \delta z)$ The component $S_{i,j}$ of the stress tensor $\mathbf{S}$ is the force per unit area in the jth direction acting across an area element whose normal is in the ith direction Forces in the direction of the normal to an area element are associated with shear stresses. Newton's third law implies that forces of equal magnitude and opposite direction act on the "plus" sides due to the matter on the "minus" sides Adding these forces, the net force on the fluid element in the jth direction is

$$\begin{aligned}\delta F_j &= S_{1j}(x+\delta x/2, y, z)\delta y\delta z - S_{1j}(x-\delta x/2, y, z)\delta y\delta z + \\ &\quad S_{2j}(x, y+\delta y/2, z)\delta x\delta z - S_{2j}(x, y-\delta y/2, z)\delta x\delta z + \\ &\quad S_{3j}(x, y, z+\delta z/2)\delta x\delta y - S_{3j}(x, y, z-\delta z/2)\delta x\delta y \qquad (17)\end{aligned}$$

Expanding each element of the stress tensor about the center of the element and keeping only the leading terms gives

$$\delta F_j = \left(\frac{\partial S_{1j}(x,y,z)}{\partial x} + \frac{\partial S_{2j}(x,y,z)}{\partial y} + \frac{\partial S_{3j}(x,y,z)}{\partial z}\right)\delta x\delta y\delta z \qquad (18)$$

Hence the force per unit volume acting at a point in the fluid due to stresses within the fluid is the divergence of the stress tensor,

$$\frac{\delta \mathbf{F}}{\delta V} = \nabla\ \mathbf{S}. \qquad (19)$$

The stress tensor is always symmetric and can be decomposed into portions due to the pressure p and the symmetric shear stress tensor T_{ij},

$$S_{ij} = -\delta_{ij}p + T_{ij} \tag{20}$$

Then the most general form of the equation of motion for the velocity vector field $\mathbf{u}$ is

$$\frac{\partial \mathbf{u}}{\partial t} + \mathbf{u} \cdot \nabla \mathbf{u} + \frac{1}{\rho}\nabla p = \frac{1}{\rho}\nabla \cdot \mathbf{T}. \tag{21}$$

A Newtonian fluid is defined as one in which the shear stress tensor is a linear function of the rate of strain tensor, where we define the symmetric rate of strain tensor as

$$R_{ij} = (\frac{\partial u_i}{\partial x_j} + \frac{\partial u_j}{\partial x_i}). \tag{22}$$

The most general linear isotropic (direction independent) relationship between the symmetric shear stress tensor $\mathbf{T}$ and the symmetric rate of strain tensor $\mathbf{R}$ is

$$\mathbf{T} = \alpha \mathbf{R} + \beta Tr(\mathbf{R})\mathbf{I}, \tag{23}$$

where $\mathbf{I}$ is the unit tensor and the constants α and β are material parameters. The components of the viscous force per unit volume are

$$(\nabla \cdot \mathbf{T})_i = \alpha \Delta u_i + (2\beta + \alpha)\frac{\partial}{\partial x_i}\nabla \cdot \mathbf{u} \tag{24}$$

Together with the condition of incompressibility, (21), becomes the *incompressible Navier-Stokes equations*

$$\frac{\partial \mathbf{u}}{\partial t} + \mathbf{u} \cdot \nabla \mathbf{u} + \frac{1}{\rho}\nabla p = \nu \Delta \mathbf{u}, \tag{25}$$

$$\nabla \cdot \mathbf{u} = 0. \tag{26}$$

The material parameter ν is the kinematic viscosity As with the incompressible Euler equations, the Navier-Stokes equations are four coupled nonlinear partial differential equations for four unknown functions: the three components of $\mathbf{u}$ and the pressure p Compared to the incompressible Euler equations, the effect of the linear coupling between stress and rate of strain is to introduce the "diffusion" term in (30)

Suppose the fluid is confined to a fixed region of space Ω bounded by $\partial\Omega$ Not only the normal component of the velocity vector field must vanish on the boundary, as it does in the boundary condition for the Euler equations in 16, but also the tangential components of the fluid's velocity are controlled. These "no-slip" boundary conditions for rigid boundaries are that the fluid at $\partial\Omega$ must move with the prescribed boundary motion. If the velocity of the boundary is given by $\mathbf{U}(\mathbf{x}, t)$ for $\mathbf{x} \in \partial\Omega$, then the appropriate boundary conditions for $\mathbf{u}$ are

$$\mathbf{u}|_{\partial\Omega} = \mathbf{U} \tag{27}$$

If an external body force (per unit volume) $\mathbf{f}$ is imposed on the fluid, then the incompressible Navier-Stokes equations become

$$\frac{\partial \mathbf{u}}{\partial t} + \mathbf{u} \cdot \nabla \mathbf{u} + \frac{1}{\rho}\nabla p = \nu \Delta \mathbf{u} + \frac{1}{\rho}\mathbf{f}, \tag{28}$$

$$\nabla \cdot \mathbf{u} = 0. \tag{29}$$

Chapter 3
Projection Method

§3.1 Projection Method

We consider the time dependent Incompressible Navier-Stokes Equations in primitive variable formulation, which were derived in the previous chapter

$$\frac{\partial \mathbf{u}}{\partial t} + \mathbf{u} \cdot \nabla \mathbf{u} + \frac{1}{\rho} \nabla p = \nu \Delta \mathbf{u} + \frac{1}{\rho} \mathbf{f}, \tag{30}$$

$$\nabla \cdot \mathbf{u} = 0, \tag{31}$$

where Ω is an open bounded domain in R^d $(d = 2, 3)$ with a sufficiently smooth boundary Γ

The equations (30) and (31) should be completed with appropriate boundary conditions for the velocity.

As with incompressible ideal flow, the pressure p in incompressible viscous flow is determined through the equation $\nabla \cdot \mathbf{u} = 0$. We now shall explore the role of the pressure in incompressible flow in more depth. Let Ω be a region in space (or in the plane) with smooth boundary $\partial\Omega$ We claim the following decomposition theorem

Theorem *Any vector field* $\mathbf{w}$ *can be uniquely decomposed in the form*

$$\mathbf{w} = \mathbf{u} + \nabla p, \tag{32}$$

where $\mathbf{u}$ *has zero divergence and is parallel to* $\partial\Omega$*; i.e.,* $\mathbf{u} \cdot \mathbf{n} = 0$ *on* $\partial\Omega$

Proof First of all we establish the orthogonality relation

$$\int_{\Omega} \mathbf{u} \cdot \nabla p \, dV = 0. \tag{33}$$

By the identity

$$\nabla(p\mathbf{u}) = (\nabla \mathbf{u})p + \mathbf{u} \cdot \nabla p, \tag{34}$$

the Divergence Theorem, and $\nabla \cdot \mathbf{u} = 0$, we get

$$\int_{\Omega} \mathbf{u} \cdot \nabla p \, dV = \int_{\Omega} \nabla(p\mathbf{u}) \, dV = \int_{\partial\Omega} p\mathbf{u} \cdot \mathbf{n} \, dA = 0, \tag{35}$$

since $\mathbf{u} \cdot \mathbf{n} = 0$ on $\partial\Omega$. We use this orthogonality to prove uniqueness. Suppose that $\mathbf{w} = \mathbf{u_1} + \nabla p_1 = \mathbf{u} + \nabla p_2$. Then

$$0 = \mathbf{u}_1 - \mathbf{u}_2 + \nabla(p_1 - p_2). \tag{36}$$

Taking the inner product with $\mathbf{u}_1 - \mathbf{u}_2$ and integrating, we get

$$0 = \int_{\Omega} \{||\mathbf{u}_1 - \mathbf{u}_2||^2 + (\mathbf{u}_1 - \mathbf{u}_2) \;\; \nabla(p_1 - p_2)\} \, dV = \int_{\Omega} ||\mathbf{u}_1 - \mathbf{u}_2||^2 \, dV \tag{37}$$

by the orthogonality relation. It follows that $\mathbf{u_1} = \mathbf{u_2}$ and $\nabla p_1 = \nabla p_2$, which is the same thing as $p_1 = p_2 + contant$. If $\mathbf{w} = \mathbf{u} + \nabla p$, we notice that $\nabla \cdot \mathbf{w} = \nabla \cdot \nabla p = \Delta p$ and that $\mathbf{w} \cdot \mathbf{n} = \mathbf{n} \cdot \nabla p$. We use this remark to prove existence Given $\mathbf{w}$ let p be defined by the solution of the Neumann problem

$$\Delta p = \nabla \cdot \mathbf{w} \quad \text{in } \Omega \qquad \text{with} \quad \frac{\partial p}{\partial n} = \mathbf{w} \cdot \mathbf{n} \quad \text{on } \partial\Omega. \tag{38}$$

It is known [7] that the solution to this problem exists and is unique up to the addition of a constant to p. With this choice of p, define $\mathbf{u} = \mathbf{w} - \nabla p$. Then clearly $\mathbf{u}$ has the desired properties $\nabla \cdot \mathbf{u} = 0, \mathbf{u} \cdot \mathbf{n} = 0$ by construction of p

It is natural to introduce the operator $\mathcal{P}$, an orthogonal projection operator, which maps $\mathbf{w}$ onto its divergence-free part $\mathbf{u}$ By the preceding theorem, $\mathcal{P}$ is well defined Notice that by construction $\mathcal{P}$ is a linear operator and that

$$\mathbf{w} = \mathcal{P}\mathbf{w} + \nabla p \tag{39}$$

$$\mathcal{P}\mathbf{u} = \mathbf{u} \text{ if } \nabla \cdot \mathbf{u} = 0, \quad \mathbf{u} \cdot \mathbf{n} = 0, \quad \text{and } \mathcal{P}(\nabla p) = 0 \tag{40}$$

We apply these ideas to the incompressible Navier-Stokes equations. If we apply the operator $\mathcal{P}$ to both sides, after rearrangement of convective term and pressure term, we obtain

$$\mathcal{P}(\frac{\partial \mathbf{u}}{\partial t} + \nabla p) = \mathcal{P}(-(\mathbf{u} \cdot \nabla)\mathbf{u} + \frac{1}{Re}\Delta \mathbf{u}) \tag{41}$$

Since $\mathbf{u}$ is divergence-free and vanishes on the boundary, the same is true of $\partial_t \mathbf{u}$(if $\mathbf{u}$ is smooth enough). Thus, by (40), $\mathcal{P}\partial_t \mathbf{u} = \partial_t \mathbf{u}$. Since $\mathcal{P}(\nabla p) = 0$, we get

$$\frac{\partial \mathbf{u}}{\partial t} = \mathcal{P}(-(\mathbf{u} \quad \nabla)\mathbf{u} + \frac{1}{Re}\Delta \mathbf{u}). \tag{42}$$

Although $\Delta \mathbf{u}$ is divergence free, it need not be parallel to the boundary and so we cannot simply write $\mathcal{P}\Delta \mathbf{u}$ This form, (42), of the Navier-Stokes equations eliminates the pressure and expresses $\partial_t \mathbf{u}$ in terms of $\mathbf{u}$ alone The pressure can then be recovered as the gradient part of $-(\mathbf{u} \cdot \nabla)\mathbf{u} + \frac{1}{Re}\Delta \mathbf{u}$ This form is not only of theoretical interest, shedding light on the role of pressure, but is of practical interest for numerical algorithms [6]

Typical initial and boundary conditions [3] involve specifying an initial velocity field and specifying *Dirichlet* or *Neumann* conditions for velocity, no boundary conditions are required for pressure Orthogonality of the pressure gradient with divergence-free vector fields effectively eliminates pressure from the system while

enforcing (31), in fact specifying pressure boundary conditions over-determines the system

§3.2 Numerical Approximation – Fractional Step

In this section, we present a variant of the fractional-step method introduced by Chorin[4] for time advancement of the Navier-Stokes and continuity equations for incompressible flows

The fractional step, or time-spitting method, is in general a method of approximation of the evolution equations based on decomposition of the operators they contain A historical review of fractional step method can be found in the book of Yanenko [25]

In application of this method to the Navier-Stokes equations, we use the interpretation that pressure plays the role of a projection operator which projects an arbitrary field into a divergence-free vector field A two step time-advancement scheme for equations (30) and (31) can be written as

$$\frac{\hat{\mathbf{u}} - \mathbf{u}^{\mathbf{n}}}{\Delta t} + (\mathbf{u} \cdot \nabla \mathbf{u})^* = \nu \Delta \mathbf{u}^* + \frac{1}{\rho}\mathbf{f}^*, \tag{43}$$

$$\frac{\mathbf{u}^{n+1} - \hat{\mathbf{u}}}{\Delta t} = -\nabla(p^{n+1}) \tag{44}$$

with

$$\nabla \quad \mathbf{u}^{n+1} = 0 \tag{45}$$

In the first step, equation (43), an auxiliary field $\hat{\mathbf{u}}$ is introduced and evaluated. $\hat{\mathbf{u}}$ differs from $\mathbf{u}^{n+1}$ because the pressure term and the continuity equation (31) have not been taken into account $\hat{\mathbf{u}}$, $\mathbf{u}^*$ and $\mathbf{f}^*$ may be evaluated by an implicit or an explicit scheme.

In the second step, equations (44) and (45) can be solved as a coupled system of equations for $\mathbf{u}^{n+1}$ and p^{n+1} with prescribed boundary condition for $\mathbf{u}^{n+1}$. To do this, Chorin [4] introduced an iteration scheme. In the present study we decouple them in the following manner, by taking the divergence on both sides of equation (44),

$$\nabla^2 p^{n+1} = \frac{1}{\Delta t} \nabla \cdot \hat{\mathbf{u}} \tag{46}$$

$$\mathbf{u}^{n+1} = \hat{\mathbf{u}} - \Delta t \nabla p^{n+1} \tag{47}$$

Chapter 4

A Numerical Method for Incompressible Navier-Stokes Equations

In this chapter, a numerical method for computing three-dimensional, time-dependent incompressible flows is presented This method is based on a fractional-step, or time-splitting, scheme in conjunction with the implicit approximate-factorization technique. The pressure Poisson equation is solved by point or line Gauss-Seidel iteration with successive over-relaxation (SOR) acceleration. Appropriate boundary conditions for the intermediate velocity field are derived.

§4.1 Temporal Discretization

We consider the implicit time advancement scheme for the advection-diffusion equations in divergence form:

$$\frac{\partial \mathbf{u}}{\partial t} = -\nabla \quad (\mathbf{uu} - \frac{1}{Re}\nabla \mathbf{u}). \tag{48}$$

We discretize the equations (48) in time by finite difference and obtain a semi-discretized form as follows

$$\frac{\hat{\mathbf{u}} - \mathbf{u}^n}{\Delta t} = -\nabla \cdot (\mathbf{uu})^n + \frac{1}{Re}[(1-\theta)\nabla^2 \mathbf{u}^n + \theta \nabla^2 \hat{\mathbf{u}}] + O(\Delta t), \tag{49}$$

where $0 < \theta < 1$ $\theta = 0$ leads to an explicit scheme. If $\theta = 0\ 5$, we have the *trapezoidal formula* . When $\theta = 1\ 0$, the equation becomes the implicit *Euler* method The function $\mathbf{u}(t) = \mathbf{u}(n\Delta t) = \mathbf{u}^n$ is assumed to be a solution of the partial differential equation (48) For convenience, we drop the error term in the rest of this section.

In 1970s, Beam-Warming [1], [2], developed an efficient non-iterative alternating-direction-implicit (ADI) method to reduce the computational cost This method

has been successfully applied to solutions of compressible Navier-Stokes equations and Euler equations.

For convenience, we rewrite the equation (48) and (49) as follows with $\mathbf{u} = (u, v, w)$

$$\frac{\partial u}{\partial t} = -\nabla \quad (u\mathbf{u} - \frac{1}{Re}\nabla u), \tag{48a}$$

$$\frac{\partial v}{\partial t} = -\nabla \cdot (v\mathbf{u} - \frac{1}{Re}\nabla v), \tag{48b}$$

$$\frac{\partial w}{\partial t} = -\nabla \quad (w\mathbf{u} - \frac{1}{Re}\nabla w), \tag{48c}$$

and

$$\frac{\hat{u} - u^n}{\Delta t} = -\nabla \cdot (u\mathbf{u})^n + \frac{1}{Re}[(1-\theta)\nabla^2 u^n + \theta\nabla^2 \hat{u}], \tag{49a}$$

$$\frac{\hat{v} - v^n}{\Delta t} = -\nabla \quad (v\mathbf{u})^n + \frac{1}{Re}[(1-\theta)\nabla^2 v^n + \theta\nabla^2 \hat{v}], \tag{49b}$$

$$\frac{\hat{w} - w^n}{\Delta t} = -\nabla \cdot (w\mathbf{u})^n + \frac{1}{Re}[(1-\theta)\nabla^2 w^n + \theta\nabla^2 \hat{w}] \tag{49c}$$

We will restrict our attention to (49a) and apply Beam-Warming's method to it The extension of this method to (49b) and (49c) is similar

We first linearize the flux function

$$\hat{f} = f(\hat{u}, \nabla\hat{u}) \tag{50}$$

by using the local Taylor expansion

$$\hat{f} = f^n + (\frac{\partial f}{\partial t})^n \delta t + O(\delta t^2) \tag{51}$$

The chain rule yields

$$\frac{\partial f}{\partial t} = \frac{\partial f}{\partial u}\frac{\partial u}{\partial t} + \frac{\partial f}{\partial(\nabla u)}\frac{\partial(\nabla u)}{\partial t}. \tag{52}$$

Notice, for the viscous flux, we have $f_{vis} = f_{vis}(\nabla u) = \frac{1}{Re}\nabla u$ Substituting (52) into (51), we obtain

$$\hat{f} = f^n + (\frac{\partial f}{\partial(\nabla u)})^n \delta(\nabla u) + O(\delta t^2), \tag{53}$$

where $\frac{\partial f}{\partial(\nabla u)}$ is the *Jacobian*

Let $\delta u = \hat{u} - u^n$ Then equation (49a) can be written as·

$$[I - \theta\frac{\Delta t}{Re}(\partial_x \mathcal{M}_1 + \partial_y \mathcal{M}_2 + \partial_z \mathcal{M}_3)]\delta u = \Delta t \mathcal{R}^n, \tag{54}$$

where I is the identity operator, and

$$\mathcal{R}^n = -\nabla \cdot (\mathbf{u}u)^n + \frac{1}{Re}(\Delta u)^n, \tag{55}$$

and

$$\mathcal{M}_1 = \frac{\partial}{\partial x} \qquad \mathcal{M}_2 = \frac{\partial}{\partial y} \qquad \mathcal{M}_3 = \frac{\partial}{\partial z} \tag{56}$$

The role of the implicit spatial operator in the left-hand-side ($\theta \neq 0$) can be interpreted as a stabilizer added to the explicit scheme, where $\theta = 0$ A general discussion of the implicit stabilization method can be found in Yanenko [25] On the other hand, this scheme can be viewed as a two-step method, with an explicit predictor plus an implicit corrector [1]

Beam and Warming [1] designed an Approximate Factorization technique by adding a small $O(\Delta t^3)$ term to the left-hand-side to factorize a n-dimensional implicit operator in equation (49a) into the product of n one dimensional implicit operators Thus equation (54) can be rewritten as:

$$(I - \theta\frac{\Delta t}{Re}\partial_x\mathcal{M}_1)(I - \theta\frac{\Delta t}{Re}\partial_y\mathcal{M}_2)(I - \theta\frac{\Delta t}{Re}\partial_z\mathcal{M}_3)\delta u = \Delta t\mathcal{R}^n \tag{57}$$

These implicit operators can be inverted in the following sequence

$$(I - \theta\frac{\Delta t}{Re}\partial_x\mathcal{M}_1)\delta\bar{u} = \Delta t\mathcal{R}^n, \tag{57a}$$

$$(I - \theta\frac{\Delta t}{Re}\partial_y\mathcal{M}_2)\delta\tilde{u} = \delta\bar{u}, \tag{57b}$$

$$(I - \theta\frac{\Delta t}{Re}\partial_z\mathcal{M}_3)\delta u = \delta\tilde{u}, \tag{57c}$$

$$\hat{u} = u^n + \delta u \tag{57d}$$

§4.2 Spatial Discretization

Now we consider the discretization of the spatial operators in equations (57a) to (57d)

In the right-hand-side of (57a), both the first and second derivatives are approximated by standard, second-order accurate, central difference Thus we obtain the residual $\mathcal{R}^n$ as

$$\begin{aligned}
\text{conv} \;=\; & \frac{1}{\Delta x}(u_{i+1,j,k}u_{i+1,j,k} - u_{i-1,j,k}u_{i-1,j,k}) + \\
& \frac{1}{\Delta y}(u_{i,j+1,k}v_{i,j+1,k} - u_{i,j-1,k}v_{i,j-1,k}) + \\
& \frac{1}{\Delta z}(u_{i,j,k+1}w_{i,j,k+1} - u_{i,j,k-1}w_{i,j,k-1}) \;,
\end{aligned} \tag{58}$$

$$
\begin{aligned}
\text{visc} &= \frac{1}{\Delta x^2}(u_{i+1,j,k} + u_{i-1,j,k} - 2u_{i,j,k}) + \\
&\quad \frac{1}{\Delta y^2}(u_{i,j+1,k} + u_{i,j-1,k} - 2u_{i,j,k}) + \\
&\quad \frac{1}{\Delta z^2}(u_{i,j,k+1} + u_{i,j,k-1} - 2u_{i,j,k}) \ ,
\end{aligned} \tag{59}
$$

$$
\mathcal{R}^n_{i,j,k} = \Delta t(-\frac{1}{2}\text{conv} + \frac{1}{Re}\text{visc}) \tag{60}
$$

In this section u^n is replaced by $u^n_{i,j,k}$, where $x = i\Delta x,\ y = j\Delta y,\ z = k\Delta z$

The second-order central difference is used to approximate the spatial differential operator in the left-hand-side Hence we have the following coupled linear algebra system

$$
c_1\delta u_{i-1} + c_2\delta u_i + c_3\delta u_{i+1} = \mathcal{R}^n_i, \tag{61}
$$

where

$$
c_1 = -\theta\frac{\Delta t}{Re\Delta x^2}, \tag{62}
$$

$$
c_2 = 1 + 2\theta\frac{\Delta t}{Re\Delta x^2}, \tag{63}
$$

$$
c_3 = -\theta\frac{\Delta t}{Re\Delta x^2}. \tag{64}
$$

Thus a huge matrix inversion problem is reduced to a series of small bandwidth (tridiagonal) matrix inversion problems that have efficient solution algorithm, e g *Thomas* algorithm

§4.3 Solution of the Pressure Poisson Equation

We apply the second-order central difference to the Laplacian in the pressure Poisson equation to obtain a discretized form as follows

$$\begin{aligned}\mathcal{L}(\phi_{i,j,k}) = \; & \tfrac{1}{\Delta x^2}(\phi_{i+1,j,k} - 2\phi_{i,j,k} + \phi_{i-1,j,k}) + \\ & \tfrac{1}{\Delta y^2}(\phi_{i,j+1,k} - 2\phi_{i,j,k} + \phi_{i,j-1,k}) + \\ & \tfrac{1}{\Delta z^2}(\phi_{i,j,k+1} - 2\phi_{i,j,k} + \phi_{i,j,k-1}) = \; s_{i,j,k},\end{aligned} \tag{65}$$

where

$$s_{i,j,k} = \frac{1}{\Delta t}\mathcal{D}(\hat{\mathbf{u}}_{i,j,k}), \tag{66}$$

and

$$\begin{aligned}\mathcal{D}(\hat{\mathbf{u}}_{i,j,k}) = & \frac{1}{2\Delta x}(u_{i+1,j,k} - u_{i-1,j,k}) \\ & + \frac{1}{2\Delta y}(v_{i,j+1,k} - v_{i,j-1,k}) \\ & + \frac{1}{2\Delta z}(w_{i,j,k+1} - w_{i,j,k-1})\end{aligned} \tag{67}$$

Here $\mathcal{L}$ and $\mathcal{D}$ are the discrete approximation of Laplacian and divergence operator

Standard point Gauss-Seidel iteration is employed. Thus equation (65) can be rewritten as

$$\begin{aligned}2(d_1 + d_2 + d_3)\phi^{n+1}_{i,j,k} = \; & d_1(\phi^{n}_{i+1,j,k} + \phi^{n+1}_{i-1,j,k}) + \\ & d_2(\phi^{n}_{i,j+1,k} + \phi^{n+1}_{i,j-1,k}) + \\ & d_3(\phi^{n}_{i,j,k+1} + \phi^{n+1}_{i,j,k-1}) - \; s_{i,j,k},\end{aligned} \tag{68}$$

where

$$d_1 = \frac{1}{\Delta x^2} \quad d_2 = \frac{1}{\Delta y^2} \quad d_3 = \frac{1}{\Delta z^2} \tag{69}$$

Alternatively, using the line Gauss-Seidel iteration, equation (68) is slightly modified as

$$\begin{aligned} 2(d_1 + d_2 + d_3)\phi^{n+1}_{i,j,k} = \; & d_1(\phi^{n+1}_{i+1,j,k} + \phi^{n+1}_{i-1,j,k}) + \\ & d_2(\phi^{n}_{i,j+1,k} + \phi^{n+1}_{i,j-1,k}) + \\ & d_3(\phi^{n}_{i,j,k+1} + \phi^{n+1}_{i,j,k-1}) + \quad s_{i,j,k}, \end{aligned} \tag{70}$$

where ϕ^{n+1} can be obtained by Thomas algorithm

After each iteration, we accelerate the convergence by successive over-relaxation as follows

$$\phi^{new} = \omega\phi^{n+1} + (1-\omega)\phi^{n}, \tag{71}$$

where $1 \leq \omega \leq 2$. An alternative is the successive under-relaxation, $0 \leq \omega \leq 1$, which assure the convergence. In our computation, we fix $\omega = 1.35$

§4.4 Solution of ϵ Advection Equation

For flows with free surfaces, several methods have been developed for numerical simulations One of most widely used is due to Hirt and Nichols [13], which is based on the concept of a fractional volume of fluid (VOF). This method has been shown to be flexible and efficient for treating complicated free boundary configurations We briefly describe this method in this section. A more detailed description can be found in [13].

Suppose that we define a function ϵ whose value is unity at any point occupied by fluid and zero otherwise. The average value of ϵ in a cell would represent the

fractional volume of the cell occupied by fluid In particular, a unit value of ϵ would correspond to a cell full of fluid, while a zero value would indicate that the cell contains no fluid Cells with ϵ values between zero and one must then contain a free surface

The time dependence of ϵ is governed a first order kinematic hyperbolic equation as follows

$$\frac{\partial \epsilon}{\partial t} + \mathbf{u} \cdot \nabla \epsilon = 0 \tag{72}$$

For incompressible fluid, the ϵ advection equation can be written in conservation law form by combining equation (74) with continuity equation

$$\frac{\partial \epsilon}{\partial t} + \nabla \quad (\mathbf{u}\epsilon) = 0, \tag{73}$$

or in component form

$$\frac{\partial \epsilon}{\partial t} + \frac{\partial f}{\partial x} + \frac{\partial g}{\partial y} + \frac{\partial h}{\partial z} = 0, \tag{74}$$

where the flux functions are

$$f = \epsilon u, \qquad g = \epsilon v, \qquad h = \epsilon w. \tag{75}$$

We first consider an explicit finite-difference approximation for a 1D advection equation The higher dimensional extension of this scheme is straightforward

$$\frac{\partial \epsilon}{\partial t} + \frac{\partial f}{\partial x} = 0 \tag{76}$$

$$\epsilon_i^{n+1} = \epsilon_i^n - \lambda(\bar{f}_{i+1/2} - \bar{f}_{i-1/2}), \tag{77}$$

where $\bar{f}_{i+1/2}$ is the numerical flux with dependence

$$\bar{f}_{i+1/2} = \bar{f}(\epsilon_i, \quad \epsilon_{i+1}), \tag{78}$$

and

$$\lambda = \frac{\Delta t}{\Delta x} \tag{79}$$

We require that $\bar{f}$ satisfies the consistency condition

$$\bar{f}(\epsilon_i, \epsilon_i) = f(\epsilon_i). \tag{80}$$

A numerical flux can be constructed in the following way [12]

$$\bar{f}_{i+1/2} = \frac{1}{2}[\ f_{i+1} + f_i - \psi(\ a_{i+1/2}\ )\Delta\epsilon_{i+1/2}\ ], \tag{81}$$

where

$$f_i = f(\epsilon_i), \tag{82}$$

$$\psi(a) = |a| \tag{83}$$

The function ψ is the coefficient of numerical viscosity Note that when $a = 0$ the numerical viscosity vanishes, which leads the calculation unstable To avoid this, the following modification of ψ is introduced in [12] as

$$\psi(a) = \begin{cases} |a| & |a| \geq \delta \\ (a^2 + \delta^2)/2\delta & |a| < 0, \end{cases} \tag{84}$$

and

$$a_{i+1/2} = \begin{cases} \Delta_{i+\frac{1}{2}} f / \Delta_{i+\frac{1}{2}} \epsilon & \Delta\epsilon_{i+\frac{1}{2}} \neq 0 \\ \frac{\partial f}{\partial \epsilon}(\epsilon_i) & \Delta\epsilon_{i+\frac{1}{2}} = 0, \end{cases} \tag{85}$$

where δ is a small number $0 < \delta < 0\ 1$ The finite difference operator acting on ϵ is

$$\Delta\epsilon_{i+1/2} = \epsilon_{i+1} - \epsilon_i \tag{86}$$

Similar treatment of the fluxes in the y and z directions can be applied to equation (74)

§4.5 Boundary Conditions

In this section, we discuss the numerical implementations of boundary conditions.

4.5.1 Pressure Boundary Condition.

Since the mathematical theory says that no physical boundary conditions are required for pressure, some numerical boundary conditions must be derived in practical calculations One widely used method is to use the normal momentum equation [16] to obtain a *Neumann* boundary condition.

In the present study, the Reynolds number *Re* is relatively high So by the boundary layer theory [18], the normal momentum equation is reduced to a homogeneous *Neumann* boundary condition

$$\frac{\partial p}{\partial n} = 0 \qquad \text{on } \partial\Omega \tag{87}$$

4.5.2 Velocity Boundary conditions.

At the solid walls, the homogeneous *Dirichlet* boundary condition is specified

$$\mathbf{u} = 0 \qquad \text{on } \partial\Omega \tag{88}$$

We derived the consistent boundary condition for the intermediate velocity field as follows Summing up (43) and (44), we have

$$\frac{\mathbf{u}^{n+1}-\mathbf{u}^{n}}{\Delta t}=-\nabla\cdot(\mathbf{u}\mathbf{u})-\nabla p^{n+1}+\frac{1}{Re}\nabla^{2}\mathbf{u} \tag{89}$$

Inserting (43) into the above equation, we have

$$\frac{\mathbf{u}^{n+1}-\mathbf{u}^{n}}{\Delta t}=\frac{\hat{\mathbf{u}}-\mathbf{u}^{n}}{\Delta t}-\nabla p^{n+1} \tag{90}$$

Since at the solid walls, (88) holds for time $n\Delta t$ and $(n+1)\Delta t$, the above equation is reduced to

$$\hat{\mathbf{u}}=\mathbf{u}^{n}+\Delta t\nabla p^{n+1} \qquad \text{on } \partial\Omega. \tag{91}$$

Applying (88) to the Navier-Stokes equations, we have

$$\begin{aligned}\nabla p^{n+1}&=\nabla p^{n}+\frac{1}{Re}\nabla^{2}(\mathbf{u}^{n+1}-\mathbf{u}^{n})\\&=\nabla p^{n}+O(\Delta t/Re)\,, \qquad \text{on } \partial\mathbf{\Omega}\end{aligned} \tag{92}$$

Hence, we reach a consistent boundary condition for the intermediate velocity field as follows

$$\hat{\mathbf{u}}=\mathbf{u}^{n}+\Delta t\nabla p^{n} \qquad \text{on } \partial\Omega. \tag{93}$$

This can rewritten in its components as

$$\hat{u}^{n}=u^{n}+\Delta t\frac{\partial p^{n}}{\partial x}\,, \tag{93a}$$

$$\hat{v}^{n}=v^{n}+\Delta t\frac{\partial p^{n}}{\partial y}\,, \tag{93b}$$

$$\hat{w}=w^{n}+\Delta t\frac{\partial p^{n}}{\partial z}\,, \tag{93c}$$

where the pressure gradient at the wall is approximated by centered or one-side (upwind) finite differences.

Note that the above equations can be cast into a delta form

$$\delta u = \Delta t \frac{\partial p}{\partial x}^{n}, \tag{93a'}$$

$$\delta v = \Delta t \frac{\partial p}{\partial y}^{n}, \tag{93b'}$$

$$\delta w = \Delta t \frac{\partial p}{\partial z}^{n}, \tag{93c'}$$

which also are the desired boundary condition for the implicit operator in (57) for the advection-diffusion equations

This result is the same as the result in [14], which they derive by a different approach

Chapter 5

A Continuum Model for Convective Melting of Solid particles in Fluid

In this chapter, we present a mathematical model for two-phase flows developed by a research group in Tennessee State University [11]

§5.1 Introduction

The understanding of the phase-change characteristics of two-phase flows occurring in micro-gravity conditions is important for the safety of space applications Such problems arise in an increasing number of applications in material processing. When a medium consists of packed (or dispersed) particles melt in a flowing fuild, at least three distinctive features arise: (1) Particles experience a full range of size variation due to phase change and collision, i.e. from initially large size (may be uniform) to eventually diminishing within the melting zone, (2) There is momentum exchange between particles and fluid due to slip (relative) and particle collision, (3) Heat is transferred from fluid to particles and is strongly influenced by flow characteristics (local Peclet number), specific inter-facial areas (particle surface area per unit volume)

The coupled heat, mass and momentum transfer mechanism during convective melting is further complicated due to the presence of the Earth gravity field The density difference between fluid and solid phases causes the melting particles either to float to the fluid surface or settle down to the bottom of the fluid field The resulting individual particle motion is then interacting with that from adjacent particles through collisions This makes prediction of melting rate under non-thermal equilibrium conditions very complex Possible experiments under micro-gravity may give a way to study such complex phenomena by eliminating gravity related effects. To be able to perform such a task, it is important to identify

the main governing parameters for complete description of convective melting processes.

§5.2 Mathematical Modeling of Two-Phase Flows

The volume-averaged equations of the continua model for multi-phase flow are [11]

$$\frac{\partial \rho^k}{\partial t} + \nabla \cdot (\rho^k \mathbf{u}_k) = S_{I-K}, \tag{94}$$

$$\frac{\partial}{\partial t}(\rho^k \mathbf{u}_k) + \nabla \cdot (\rho^k \mathbf{u}_k \mathbf{u}_k) = -\nabla p^k + \nabla \cdot \tau^k + \rho^k \mathbf{b}_k + \mathbf{F}_{I-K} + S_{I-K}\mathbf{u}_k, \tag{95}$$

$$\begin{aligned} \frac{\partial}{\partial t}(\rho^k E_k) + \nabla \cdot (\rho^k E_k \mathbf{u}_k) &= -p^k \nabla \cdot \mathbf{u}_k \\ &+ < \tilde{\tau}^k \quad \nabla \tilde{\mathbf{u}}^k > -\nabla \cdot \mathbf{q}^k + Q_{I-K} + S_{I-K}E_{I-K} + < \tilde{\Phi}^k >, \end{aligned} \tag{96}$$

where S_{I-K} represents the rate of mass generation of phase k per unit volume and may be caused by chemical reactions or phase changes. This unit 'volume' is that of the multi-phase system $\mathbf{F}_{I-K}$accounts for the transfer of the total stress across the interface per unit volume and includes the drag force, Saffman force, and Magnus force of the phase $S_{I-K}\mathbf{u}_k$ represents the momentum transfer across the interface per volume, due to the mass generation of the phase. Q_{I-K} accounts for the heat transfer across the interface. $S_{I-K}E_{I-K}$ represents the internal energy transferred by the mass generation as a result of phase change

The total stress has already been written as the form of pressure plus shear stress, $\tilde{T}^k = -\tilde{p}^k\delta + \tilde{\tau}^k$, in the above equations To solve the equations, constitutive equations, which describe the relationship between stress and dependent variables,

must be specified. In addition, the interchange terms of mass, momentum and energy is also need to be specified

For a liquid-solid two-phase system, the relationship between liquid and solid volume fraction is

$$\epsilon_l + \epsilon_s = 1. \tag{97}$$

Therefore, only one of liquid and solid volume fraction is independent variable We write $\epsilon = \epsilon_l$, then $\epsilon_s = 1 - \epsilon$

Densities of the liquid phase and the solid particle phase are

$$\rho^l = \epsilon\rho_l \qquad \rho^s = (1-\epsilon)\rho_s, \tag{98}$$

Mass generation rates of the liquid phase and the solid particle phase per unit volume are expressed as

$$S = S_{I-l} = S_{I-s} = \frac{h_p A_l}{r_s}(T_l - T_s) = \frac{h}{r_s}(T_l - T_s). \tag{99}$$

Because the solid particle phase is treated as a continuum and particles in the liquid-solid system may be treated as 'amplified molecules' in the present continuum model, the transport properties of the solid phase are needed in the model The pressure of the liquid phase and of the solid particle phase may be written as

$$p^l = \epsilon p \qquad p^s = (1-\epsilon)p + p_s, \tag{100}$$

where p_s shows the contribution to the pressure of solid phase due to the interaction between particles. Such a general formulation with proper values of material constants does not exist today. A modulus of elasticity or particle-to-particle interaction , $G(\epsilon)$, is introduced into the present continuum model of liquid-solid

two-phase system, similar to that in the hydrodynamic model for gas-solid fluidization of Pritchett et al, (1978)

$$G(\epsilon) = \frac{dp_s}{d\epsilon} \tag{101}$$

Therefore, in the solid momentum equation, we have

$$\nabla p_s = G(\epsilon)\nabla\epsilon \tag{102}$$

The modulus of elasticity may be taken as

$$G(\epsilon) = -G_0 e^{C(\epsilon^* - \epsilon)}, \tag{103}$$

where usually $G_0 = 1.0Pa$, $C = 100$, and $\epsilon^* = 0.45$. The introduction of the modulus of elasticity is necessary not only in the physical sense, but also from the need of numerical technique. This term becomes of numerical significance only when the volume fractions of liquid go below the minimum value It also helps to make the system numerically stable, because it converts the imaginary characteristics into real values. Our preliminary calculations show that it is necessary to adjust this pressure to prevent the volume fraction from reaching impossibly low values.

Shear stress tensors of the liquid phase and the solid particle phase are

$$\tau^l = \epsilon\tau_l \qquad \tau^s = (1-\epsilon)\tau_s. \tag{104}$$

The liquid and solid are assumed as Newtonian fluids as first approximation when there are no better experimental results,

$$\tau_l = \mu_l[\nabla\mathbf{u}_l + (\nabla\mathbf{u}_l)^T], \qquad \tau_s = \mu_s[\nabla\mathbf{u}_s + (\nabla\mathbf{u}_s)^T]. \tag{105}$$

Body force vectors of the liquid phase and the solid particles phase under normal condition are

$$\rho^l \mathbf{b}_l = \rho^l \mathbf{g}, \qquad \rho^s \mathbf{b}_s = \rho^s \mathbf{g} \tag{106}$$

Momentum transfer vectors across the interface per unit volume are

$$-\mathbf{F}_{I-l} = \mathbf{F}_{I-s} = \beta(\mathbf{u}_l - \mathbf{u}_s) - (1-\epsilon)D(\epsilon)\rho_l \frac{d}{dt}(\mathbf{u}_l - \mathbf{u}_s) - p\nabla\epsilon \tag{107}$$

On the right-hand side of this relation, the first term is drag force. The second term is virtual mass force, and the third term is the force caused by the gradient of volume fraction $D(\epsilon)$ is the virtual mass coefficient For dispersed spherical particles, $D(\epsilon) = 0.5$

If ϵ is less than 0 8, then the drag coefficient β is given by *Ergun*'s equation as [11]

$$\beta = 150\frac{(1-\epsilon)^2}{\epsilon}\frac{\mu_l}{(\phi_s d_p)^2} + 1\ 75(1-\epsilon)\frac{\rho_l}{(\phi_s d_p)}|\mathbf{u}_l - \mathbf{u}_s|. \tag{108}$$

If ϵ is greater than 0 8, the drag coefficient in this porosity range becomes

$$\beta = \frac{3}{4}C_d\frac{\epsilon(1-\epsilon)}{(\phi_s d_p)}\rho_l|\mathbf{u}_l - \mathbf{u}_s|\epsilon^{-2\ 625}, \tag{109}$$

where C_d is related to the *Reynolds* number by

$$C_d = \begin{cases} Re_p(1 + 0.15Re_p^{0\ 687})/24 & Re_p < 1000, \\ 0.44 & Re_p \geq 1000 \end{cases} \tag{110}$$

In equation (124), $\epsilon^{-2\ 625}$ shows the effect due to the presence of other particles in the fluid and acts as a correction to the usual *Stock* law for free fall of a single particle.

According to the thermodynamics relation of internal energy and temperature, internal energies per unit mass of the liquid phase and the solid particle phase are

$$E_l = C_{v,l}T_l, \qquad E_s = C_{v,s}T_s, \tag{111}$$

with $C_{v,i}$ the heat capacity of phase $i = l, s$, and T_i the temperature

Heat flux vectors in the liquid phase and the solid particle phase are given by *Fourier*'s law as

$$\mathbf{q}^l = -\epsilon k_{eff,l}\nabla T_l, \qquad \mathbf{q}^s = -(1-\epsilon)k_{eff,s}\nabla T_s, \tag{112}$$

where all of variables are volume-averaged, therefore the thermal conductivity are effective in the volume-average sense, as follows

$$k_{eff,l} = k_{b,l}/\epsilon, \qquad k_{eff,s} = k_{b,s}/(1-\epsilon), \tag{113}$$

where

$$k_{b,l} = (1-\sqrt{1-\epsilon})k_l, \tag{114}$$

$$k_{b,s} = (1-\epsilon)[\eta A + (1-\eta)Z]k_s, \tag{115}$$

$$Z = \frac{2}{1-B/A}[\frac{B-B/A}{(1-B/A)^2}ln(\frac{A}{B}) - \frac{B-1}{1-B/A} - \frac{1}{2}(B+1)], \tag{116}$$

$$B = 1\ 25(1/\epsilon - 1)^{10/9} \tag{117}$$

For spherical particles, $A = k_s/k_l$, and $\eta = 7\ 26 \times 10^{-3}$

Heat transfer across the interface of the liquid phase and the solid phase is

$$Q_{I-l} = -Q_{I-s} = -h(T_l - T_s), \tag{118}$$

where h is a volume convective heat transfer coefficient [11],

$$h = \frac{6(1-\epsilon)}{(\phi_s d_p)} h_p \tag{119}$$

The convective heat transfer coefficient h_p can be computed by [11]

$$Nu_p = \frac{h_p d_p}{k_l} = 2 + 1\ 1 Re_p^{0\ 6} Pr^{1/3}. \tag{120}$$

Incorporating the above relations into (a 1-3), the volume-averaged equations of mass, momentum and energy conservation can be expressed by

$$\frac{\partial}{\partial t}(\epsilon \rho_l) + \nabla \cdot (\epsilon \rho_l \mathbf{u}_l) = S, \tag{121}$$

$$\frac{\partial}{\partial t}[(1-\epsilon)\rho_s] + \nabla \cdot [(1-\epsilon)\rho_s \mathbf{u}_s] = -S, \tag{122}$$

$$\begin{aligned} &\frac{\partial}{\partial t}(\epsilon \rho_l \mathbf{u}_l) + \nabla \cdot (\epsilon \rho_l \mathbf{u}_l \mathbf{u}_l) = \\ &\quad -\epsilon \nabla p + \nabla \cdot [\epsilon \mu_l (\nabla \mathbf{u}_l + \nabla \mathbf{u}_l^T)] + \epsilon \rho_l \mathbf{g} \\ &\quad - \beta(\mathbf{u}_l - \mathbf{u}_s) + (1-\epsilon) D(\epsilon) \rho_l \frac{d}{dt}(\mathbf{u}_l - \mathbf{u}_s) + S\mathbf{u}_l, \end{aligned} \tag{123}$$

$$\begin{aligned} &\frac{\partial}{\partial t}[(1-\epsilon)\rho_s \mathbf{u}_s) + \nabla \cdot [(1-\epsilon)\rho_s \mathbf{u}_s \mathbf{u}_s) = \\ &\quad -(1-\epsilon)\nabla p - G(\epsilon)\nabla \epsilon + \nabla \cdot [(1-\epsilon)\mu_s (\nabla \mathbf{u}_s + \nabla \mathbf{u}_s^T)] + (1-\epsilon)\rho_s \mathbf{g} \\ &\quad + \beta(\mathbf{u}_l - \mathbf{u}_s) - (1-\epsilon) D(\epsilon) \rho_l \frac{d}{dt}(\mathbf{u}_l - \mathbf{u}_s) - S\mathbf{u}_s, \end{aligned} \tag{124}$$

$$\begin{aligned} &\frac{\partial}{\partial t}(\epsilon \rho_l C_{v,l} T_l) + \nabla \cdot (\epsilon \rho_l C_{v,l} T_l \mathbf{u}_l) = \\ &\quad \nabla \cdot (\epsilon k_{eff,l} \nabla T_l) - h(T_l - T_s) + S C_{v,l} T_l, \end{aligned} \tag{125}$$

$$\frac{\partial}{\partial t}[(1-\epsilon)\rho_s C_{v,s} T_s] + \nabla \cdot [(1-\epsilon)\rho_s C_{v,s} T_l \mathbf{u}_s] =$$
$$\nabla \cdot [(1-\epsilon k_{eff,s} \nabla T_s] + h(T_l - T_s) - S C_{v,s} T_s \tag{126}$$

In the thermal energy equation, the pressure terms, the dissipation function terms and the terms of *Joule*'s heating and thermal radiation usually can be neglected, as we have done

There are ten nonlinear coupled partial differential equations for ten dependent variables ϵ, u_l, v_l, w_l, u_s, v_s, w_s, T_l, T_s, p. Therefore, the set of equations with appropriate initial and boundary conditions is closed

Chapter 6
Results and Discussion

Test cases, designed to investigate the accuracy and limitations of algorithm implementations, can be grouped into three classes of problem [23]. *verification, benchmarking, and validation. Verification* involves the comparison of computational to analytical results for problems in which a " closed form" solution exists *Benchmarking* is the comparison of results to those produced by an independent computational model, i e., "code to code" comparisons. Code *validation* requires the comparison of computer simulations to experimental data. The results of test cases, selected from first two categories, are presented in this chapter with the intent of exploring the accuracy, convergence, and stability of our numerical method we developed in previous chapters .

§6.1 Two-Dimensional Developing Flows in a Duct

Two dimensional, steady state, isothermal, laminar flow in a straight duct is a widely used verification case for incompressible Navier-Stokes solvers. The flow is linear so that an exact solution can be obtained The exact solution is archived in Schlichting's book [18]

In this case, a uniform mesh is employed, with a domain

$$\Omega = \{ (x, y) \mid 0 < x < 30, \quad 0 < y < 1 \}$$

This two-dimensional domain is partitioned uniformly with $\Delta x = 0\ 1$ and $\Delta y = 0.025$ For moderate Reynolds number flows, this mesh is fine enough to resolve the velocity gradient in y direction

In this test case, we meet three kinds of boundaries, i e, inflow outflow and solid wall The boundary conditions are specified as follows for these boundaries

(a) at the inflow boundary $\partial\Omega_1 = \{ (x,y) \mid x = 0 \}$, we have the Dirichlet boundary condition

$$u = 1, \qquad v = 0 \qquad \text{on } \partial\Omega_1$$

(b) at the outflow boundary $\partial\Omega_2 = \{ (x,y) \mid x = 30 \}$, we have the Neumann boundary condition

$$\frac{\partial u}{\partial x} = 0, \qquad \frac{\partial v}{\partial x} = 0 \qquad \text{on } \partial\Omega_2$$

(c) at the solid wall boundary $\partial\Omega_3 = \{ (x,y) \mid y = 0 \text{ or } y = 1 \}$ we have the Dirichlet boundary condition

$$u = v = 0 \qquad \text{on } \partial\Omega_3.$$

The calculation starts with a uniform initial field with $u = 1$ and $v = 0$ for Re =100. We integrate the equations in time and solution goes to steady state, i e $\partial \mathbf{u}/\partial t \to 0$, as time $t \to \infty$. In practical calculation, we assume that the steady state is reached and the calculation is terminated when

$$Max|\frac{u_i^{n+1} - u_i^n}{\Delta t}| \leq 10^{-5}$$

In each time step, the Poisson equation is iterated for 500 cycles, which makes the discrete divergence small enough and discrete continuity equation satisfied When less iterations were performed, we observed the increasing mass loss in the result

Fig.1 shows our computation result of velocity profile for a flow at $Re = 50$. It is a parabola and the wall boundary layer is clearly presented

§6.2 Two-Dimensional Driven Cavity Flows

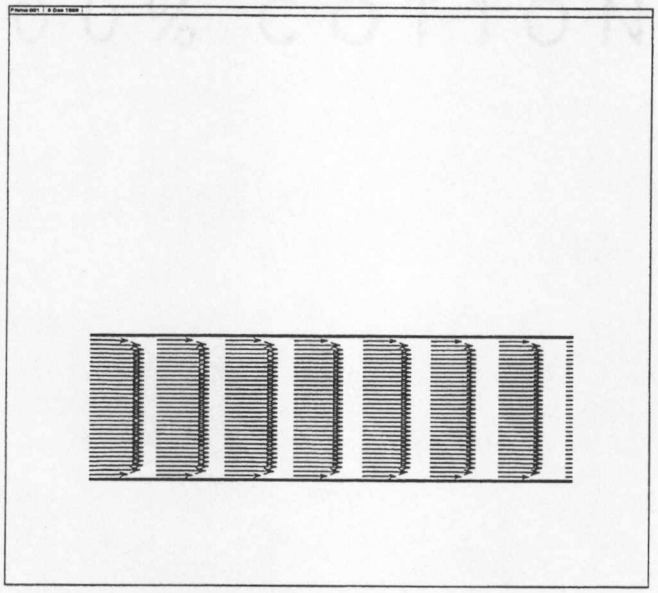

Figure 1: Velocity profile of a developed duct flow

This laminar two-dimensional driven cavity flow problem was benchmarked by Ghia et al [8].

The rectangular driven cavity is

$$\Omega = \{ \ (x, y) \mid 0 < x < 1, \ \ 0 < y < 1 \ \}.$$

It is partitioned uniformly with $\Delta x = \Delta y = 0.03125$ for flows with relatively low Reynolds number. In the calculations for Reynolds above 3200, the mesh is refined with $\Delta x = \Delta y = 0.0078125$.

Flow is driven by the lower wall. This is characterized by the boundary conditions. On the boundary $\partial\Omega_1 = \{ \ (x, y) \mid y = 0 \ \}$, we specify

$$u = 1, \quad v = 0 \qquad \text{on } \partial\Omega_1.$$

At the rest of the boundary $\partial\Omega_2 = \partial\Omega - \partial\Omega_1$, we specify

$$u = v = 0 \qquad \text{on } \partial\Omega_2.$$

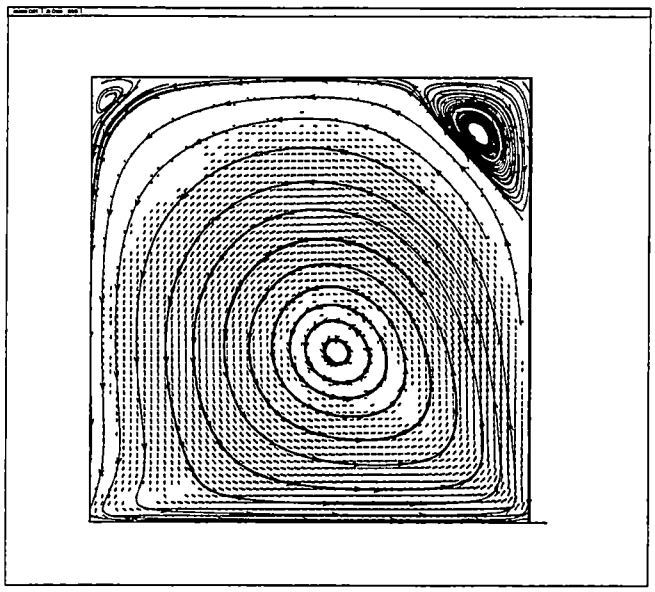

Figure 2: Velocity vector and streamlines of the driven cavity flow at Re=400

At the very beginning of the calculation, the velocity field is initialized as

$$u = v = 0, \qquad \text{in } \Omega \times \{\ t = 0\ \}$$

There are several standing vortices exist in the cavity which are highly depend on Reynolds number. At very low Reynolds number, the flow is almost symmetric with respect to the center line and two corner eddies are visible. As Reynolds number increases, the center of the main vortex moves towards the downstream corner (Fig. 2 for Re = 400, Fig. 3 for Re = 1000, Fig 4 for Re = 3200, and Fig. 5 for Re = 5000) before it returns toward the center at higher Reynolds numbers

At Reynolds number = 5000, a tertiary corner eddy is visible in Fig. 6, which shows both the velocity vector and streamline contour From the velocity vectors, a smaller eddy can also be observed in the corner, which is too weak to be displayed clearly by the streamlines

For more higher Reynolds numbers, the nonlinear convective terms are completely dominate Steady state solutions do not exist and periodic solutions are

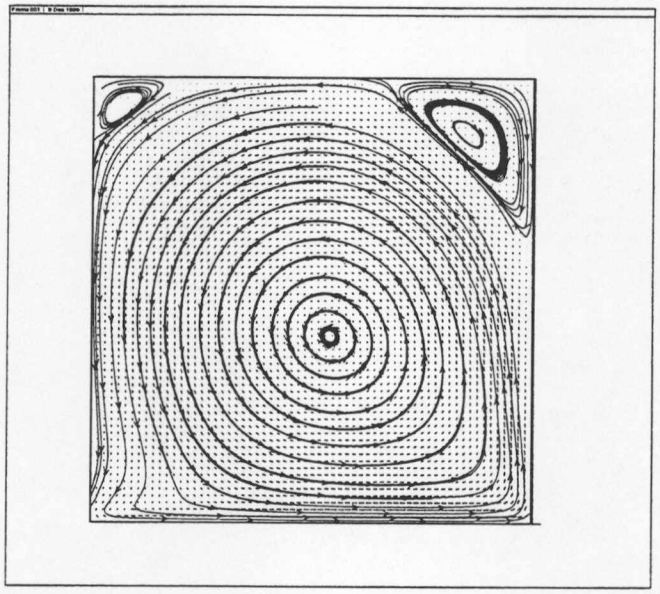

Figure 3: Velocity vector and streamlines of the driven cavity flow at Re=1000

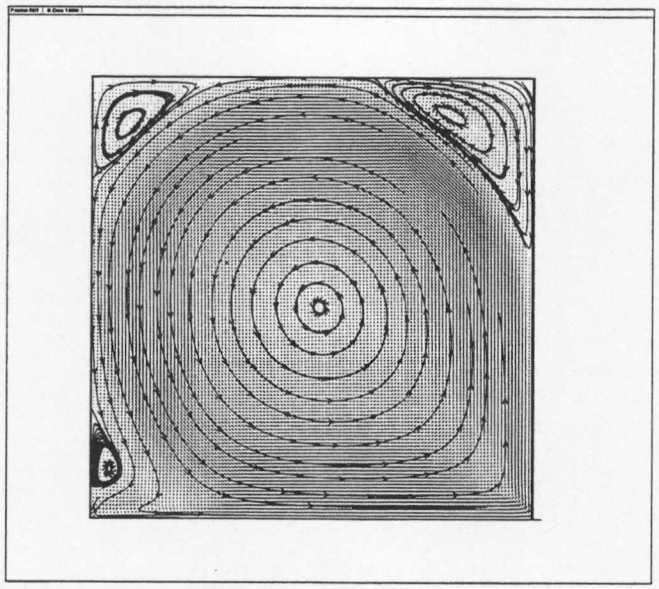

Figure 4: Velocity vector and streamlines of the driven cavity flow at Re=3200

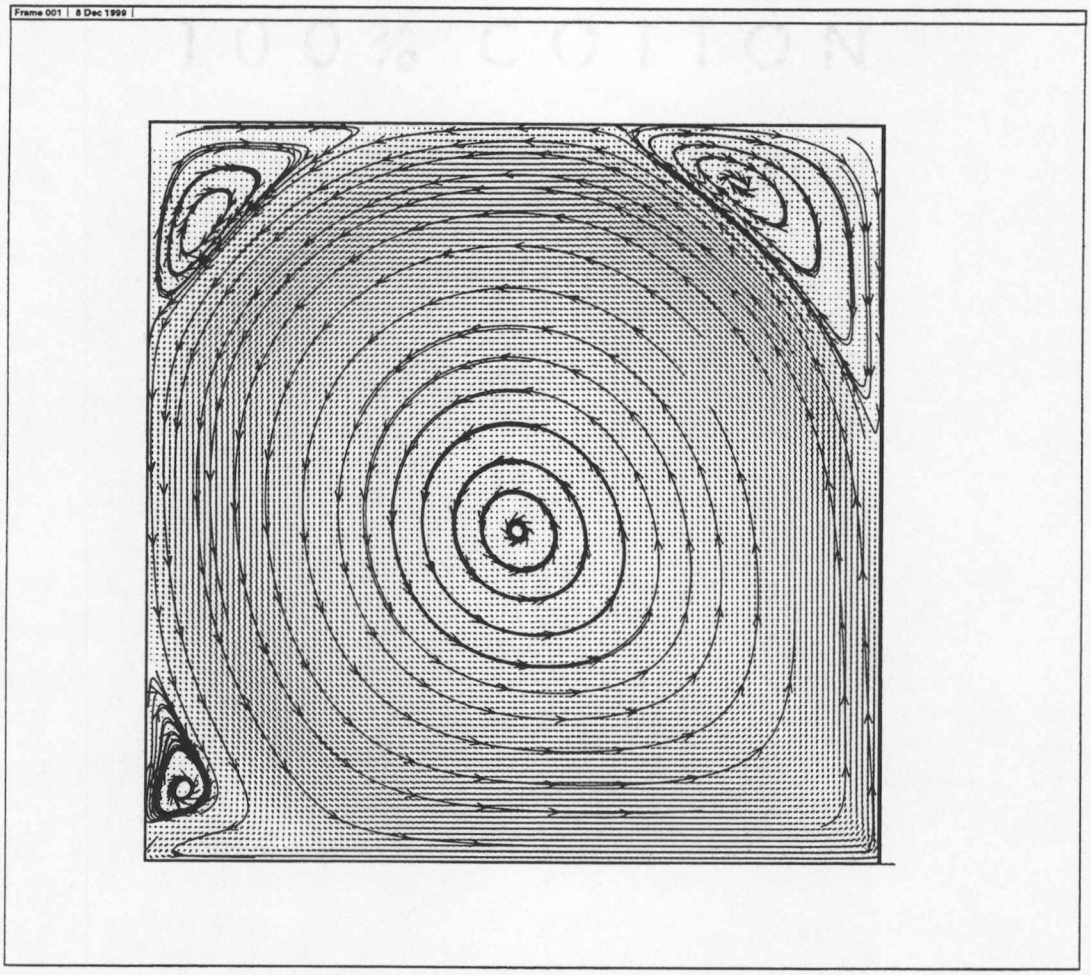

Figure 5: Velocity vector and streamlines of the driven cavity flow at Re=5000

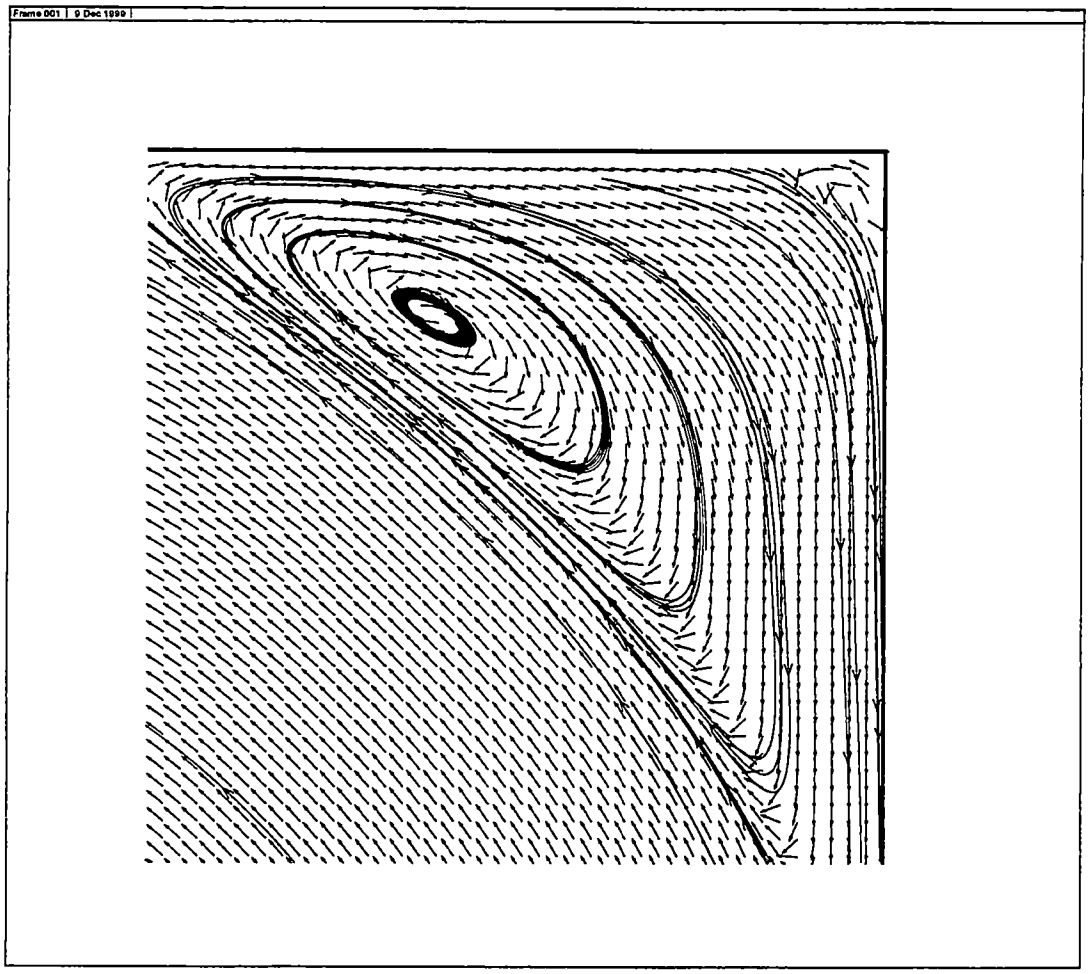

Figure 6· The tertiary corner eddy in the driven cavity flow at Re=5000

expected. As Reynolds number increases further, transition from laminar flow to turbulent flow will happen.

§6.3 Two-Dimensional Thermo Driven Cavity Flows

Buoyancy-driven flow, resulting from natural convection in an enclosed cavity, is another famous benchmark for incompressible Navier-Stokes problems This problem also has many practical applications including nuclear reactor insulation, energy conservation, ventilation of rooms, solar energy collection, etc

The problem, commonly referred to as the "double-glazing" problem, is that of two-dimensional flow of an incompressible fluid of Prandtl number 0 71 in an upright square cavity of side 1 The buoyancy body force is modeled by the Boussinesq approximation The upper and lower horizonal walls are adiabatic, and the vertical side-walls are set at the constant uniform temperature T_{hot} and T_{cold}. The velocity boundary conditions is no-slip on the four walls

In the present study, the energy equation is incorporated and calculated in each time step after the solution of the Navier-Stokes equations. The energy equation in non-dimensional form can be written as

$$\frac{\partial \mathbf{u}}{\partial t} + \mathbf{u} \cdot \nabla \mathbf{u} = -\nabla p + \frac{1}{Re}\Delta \mathbf{u} + \frac{Gr}{Re^2} T\mathbf{g}, \tag{127}$$

$$\nabla \quad \mathbf{u} = 0, \tag{128}$$

$$\frac{\partial T}{\partial t} + \nabla \cdot (\mathbf{u}T) = \frac{1}{RePr}\nabla^2 T + \frac{Ec}{Re}\Phi, \tag{129}$$

where g is the gravity vector and Φ is the dissipation function as

$$\Phi = 2[(\frac{\partial u}{\partial x})^2 + (\frac{\partial v}{\partial y})^2 + (\frac{\partial w}{\partial z})^2] + (\frac{\partial v}{\partial x} + \frac{\partial u}{\partial y})^2 + (\frac{\partial w}{\partial y} + \frac{\partial v}{\partial z})^2 + (\frac{\partial u}{\partial z} + \frac{\partial w}{\partial x})^2. \tag{130}$$

The non-dimensional parameters Re, Pr, Ec, Gr are known as Reynolds number, Prandtl number, Eckert number and Grashof number respectively. Rayleigh number is defined as $Ra = PrGr$

In this case, the computational domain is the same as that in case 2

The velocity boundary is condition is

$$\mathbf{u} = 0 \qquad \text{on } \partial\Omega,$$

For the temperature, we need to specify both Dirichlet and Neumann boundary conditions as follows

On $\partial\Omega_1 = \{ (x, y) \mid x = 0 \}$ we have

$$T = 1 \qquad \text{on } \partial\Omega_1$$

On $\partial\Omega_2 = \{ (x, y) \mid x = 1 \}$ we have

$$T = 0 \qquad \text{on } \partial\Omega_2$$

On $\partial\Omega_3 = \partial\Omega - (\partial\Omega_1 \cup \partial\Omega_2)$ we have

$$\frac{\partial T}{\partial n} = 0 \qquad \text{on } \partial\Omega_3.$$

The temperature contour for Rayleigh number of 100 are shown in Fig 7. The slight stratification the temperature field is viewed Fig 8 is the velocity vector and streamline contour, in which the primary vortex is clearly presented.

This result is compared to that reported in [23] Calculations for higher Rayleigh number cases will be carried out in future studies

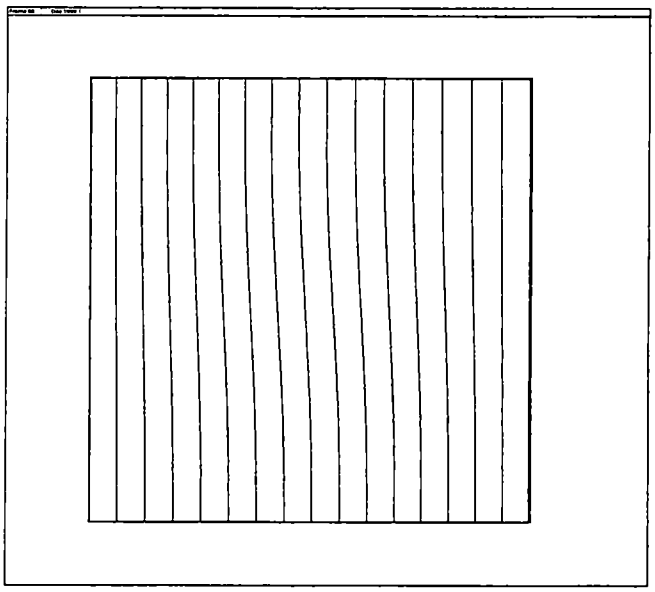

Figure 7 Temperature contour of the thermo driven cavity flow at Ra=100

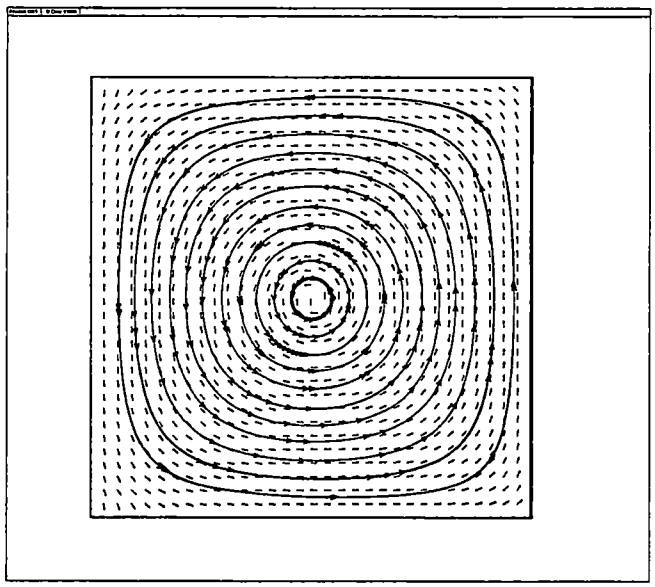

Figure 8 Velocity vector and streamlines of the thermo driven cavity flow at Ra=100

§6.4 Two-Dimensional Melting of Ice in Water

In this case, we simulate the melting of ice in water, a liquid-solid two-phase flow, by coupling the model reported in chapter 5 with the incompressible Navier-Stokes solver

The computational domain is defined as

$$\Omega = \{ \ (x, y) \mid 0 < x < 1, \ \ 0 < y < 1 \ \}$$

The boundary conditions for the liquid phase in dimensionaless variables are

$$u_l = v_l = 0 \ \text{ and } \ \frac{\partial T}{\partial n} = 0 \ \text{ on } \ y = 0 \quad \text{ and } \ y = 1,$$

$$u_l = 1, \ \ v_l = 0, \ \ T_l = 1.0733 \ \text{ on } \ x = 0$$

At the outlet boundary, we use extrapolation technique to approximate the normal derivatives,

$$\frac{\partial T_l}{\partial n} = \frac{\partial u_l}{\partial n} = \frac{\partial v_l}{\partial n} = 0.$$

For the solid phase, we have the following boundary conditions.

$$u_s = v_s = 0 \ \text{ and } \ \frac{\partial T_s}{\partial n} = 0 \ \text{ on } \ \partial\Omega$$

We initialize the flow field using

$$u_l = 1, \qquad v_l = 0, \qquad T_l = 1\ 0733, \qquad \rho_l = 1\ 0,$$

$$u_s = 0, \qquad v_s = 0, \qquad T_s = 0\ 9817, \qquad \rho_s = 0\ 917,$$

$$\epsilon = 0\ 74$$

Some flow field parameters are in the following list

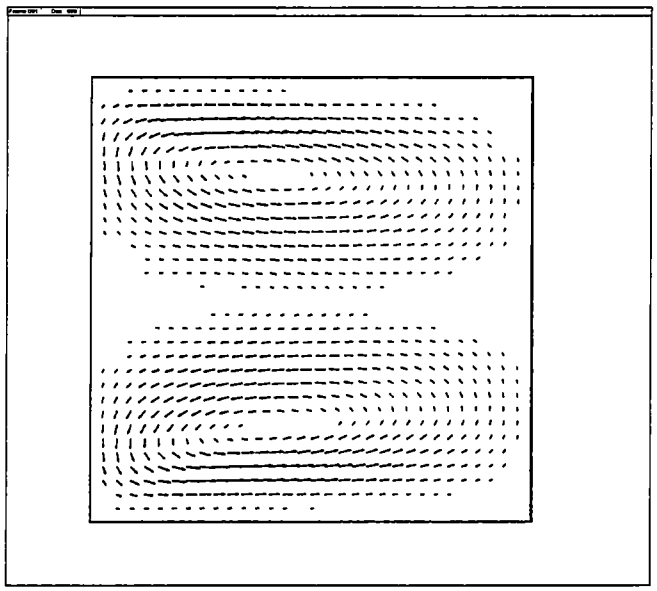

Figure 9. Velocity vector of a two-phase flow, melting of ice in water

Latent heat for fusion h_{ls}	$3.35 \times 10^5 J/kg$
Reynolds number Re_p	$\epsilon\rho_l\|\mathbf{u}_l - \mathbf{u}_s\|d_p/\mu_l$
Prandtl number Pr	7 01 .
Nusselt number Nu_p	$h_p d_p/k_l$
Paritcle diameter d_p	0 001m.
Sphericity ϕ	1
Thermal Conductivity k	$k_l = 0.617W/m\ \ K$, $k_s = 0\ 188W/m \cdot K$
Specific Heat C_v	$C_{vl} = 4184J/kg \cdot K$ $C_{vs} = 2040J/kg \cdot K$
Viscosity μ	$\mu_l = 0\ 0018N\ \ s/m^2$, $\mu_s = 0.02N \cdot s/m^2$

Fig 9 is the velocity vector plot The counterrotating vortices can be seen

In the present study, all the test cases are solved in nondimensional form without considering the real physics. In our future studies, experimental data [11] will be adopted to validate the model

§6.5 Three-Dimensional Driven Cavity Flows

In this case, we extend our calculation to three-dimensional problems by adding a spanwise direction to the two-dimensional case 2. Thus the computational domain is

$$\Omega = \{ (x, y, z) \mid 0 < x < 1, \quad 0 < y < 1, \quad 0 < z < 1 \ \}.$$

It is partitioned uniformly with $\Delta x = \Delta y = \Delta z = 0\ 03125$

The boundary condition is similar to that in case 2.

On the boundary $\partial\Omega_1 = \{ (x, y, z) \mid x = 0 \}$, we specify

$$u = 0, \quad v = 1, \quad w = 0 \qquad \text{on } \partial\Omega_1.$$

At the rest of the boundary $\partial\Omega_2 = \partial\Omega - \partial\Omega_1$, we specify

$$u = v = w = 0 \qquad \text{on } \partial\Omega_2$$

At the very beginning of the calculation, the velocity field is initialized as

$$u = v = w = 0, \qquad \text{in } \Omega \times \{ t = 0 \}$$

Since low Reynolds number flows are relatively easier to obtain, we first calculate a low Reynolds number solution, which is then used as initial field for calculation of a high Reynolds number flow In fact, the higher Reynolds number solution can be viewed as a perturbation of the lower Reynolds number solution and only a small amount of computation is needed. Thus by successively increasing the Reynolds number, the computation is accelerated significantly to reach a desired high Reynolds number solution

One characteristic of three dimensional driven cavity flows is the existence of Taylor-Gortler-type vortices, which are formed as a result of the streamline curvature owing to the primary vortex. The observation of this three-dimensional structure by numerical simulation is reported in [24]

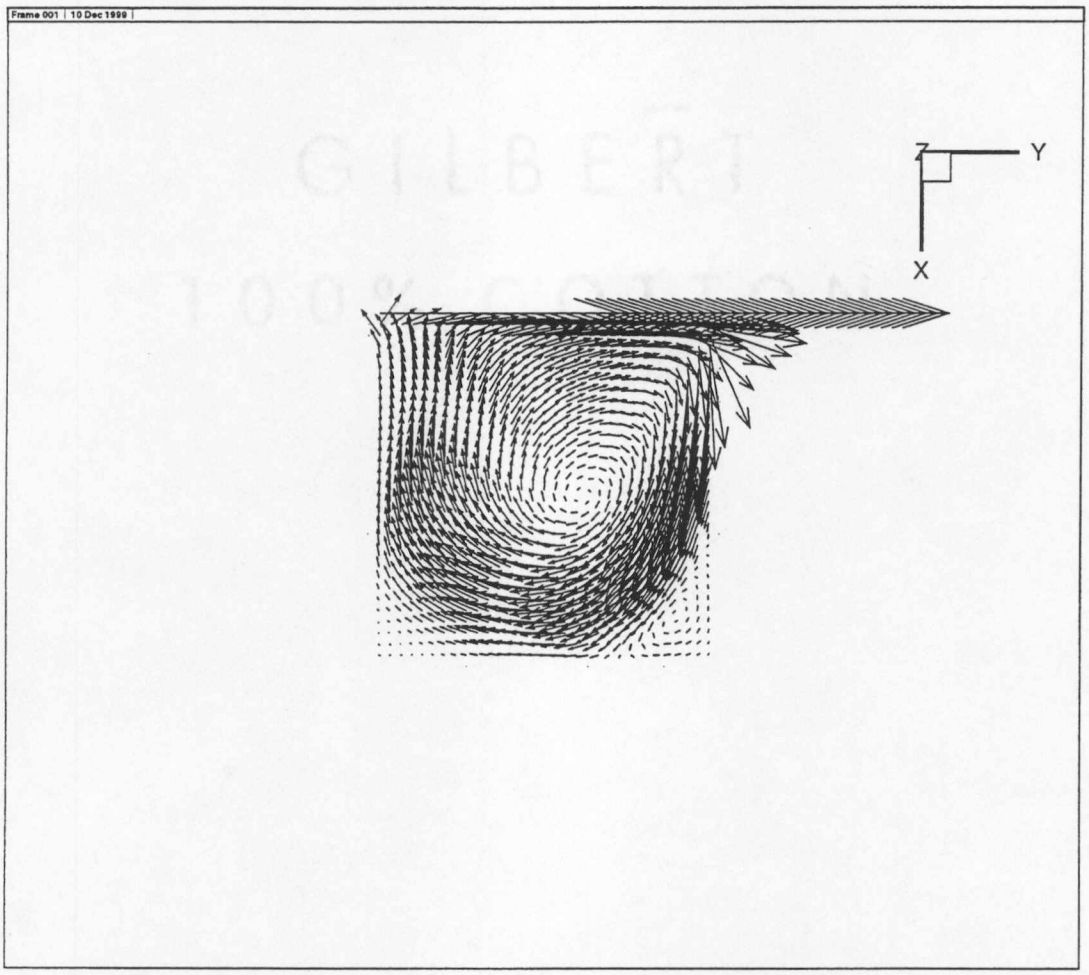

Figure 10: Velocity vector plot of the 3D driven cavity flow at z=0.5 plane

Fig. 10 show shows the primary vortex for Reynolds number of 1000 at the plane $z = 0.5$, which looks like the two-dimensional solution. Fig. 11 and Fig. 12 are the velocity vector plot at the planes $y = 0.5$ and $x = 0.5$ respectively, which are perpendicular to the primary vortex plane. These figure show the existence of a counter-rotating vortices.

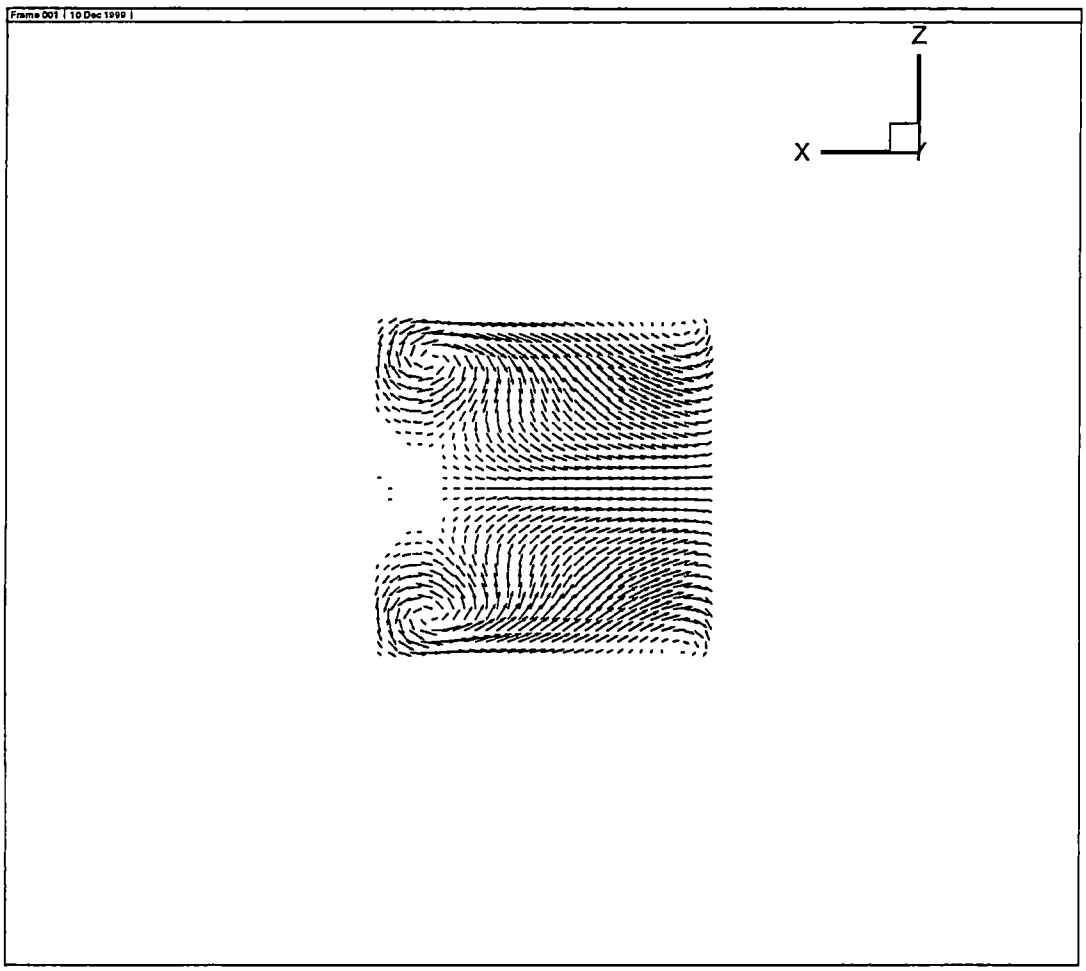

Figure 11· Velocity vector plot of the 3D driven cavity flow at y=0 5 plane

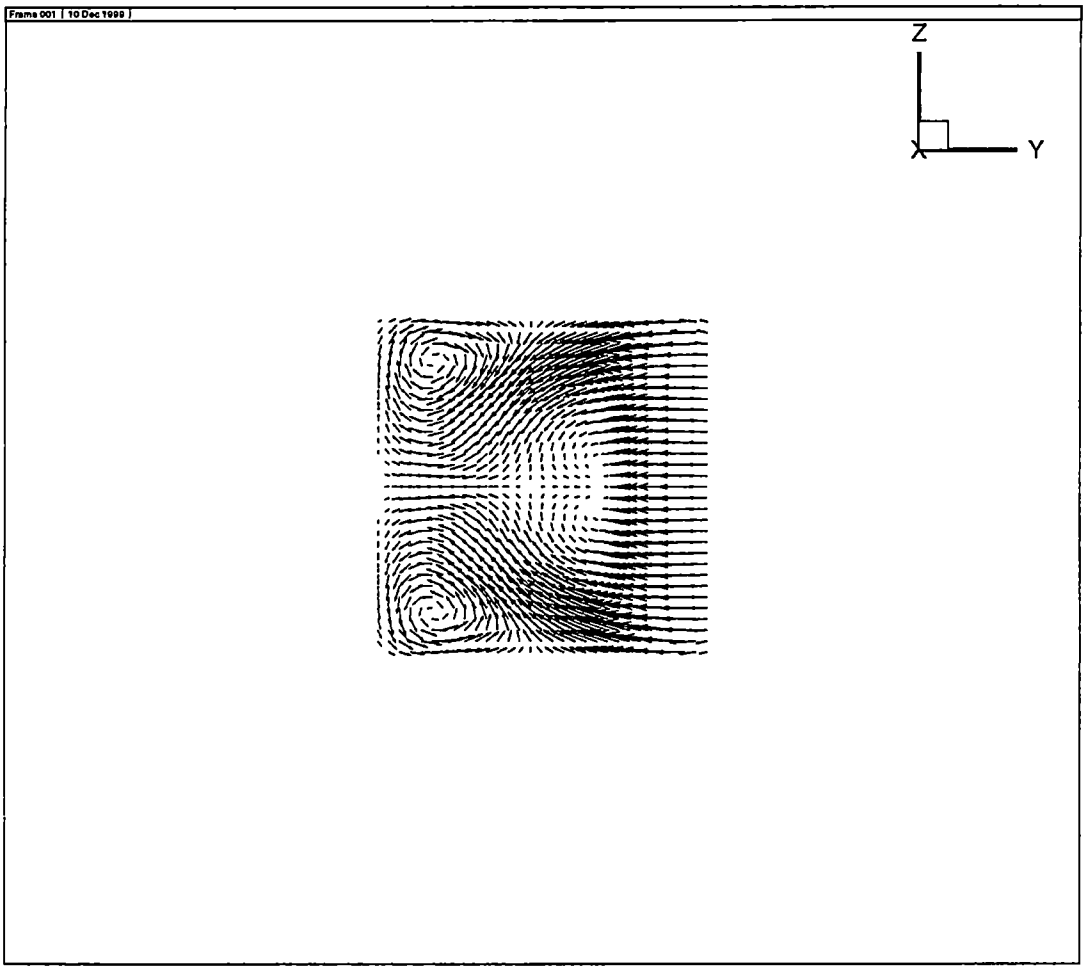

Figure 12 Velocity vector plot of the 3D driven cavity flow at x=0.5 plane

References

References

[1] Beam, R M and Warming, R F 1976, An Implicit Finite-Difference Algorithm for Hyperbolic System in Conservation-Law Form, J of Comput. Phys , vol 22, pp 87-110

[2] Beam, R M and Warming, R. F. 1978, An Implicit Factored Scheme for the Compressible Navier-Stokes Equations, J of American Institute of Aeronautics and Astronautics, vol 16, No 4, pp. 393-402.

[3] Bell, J B , Colella, P., and Glaz, H. M., 1989, A Second-Order Projection Method for the Incompressible Navier-Stokes Equations, J Comput Phys , vol 85, pp 257-283

[4] Chorin, A J , 1968, Numerical Solution of the Navier-Stokes Equations, Math of Comput , vol 22, pp 742 - 762

[5] Chorin, A J., 1969, On the Convergence of Discrete Approximations to the Navier-Stokes Equations, Math. of Comput., vol 23, pp. 341 - 353.

[6] Chorin, A. J and Marsden, J. E , 1982, A Mathematical Introduction of Fluid Mechanics, second edition, Springer-Verlag, New York

[7] Evans, L C , 1998, Partial Differential Equations, American Mathematical Society, Providence

[8] Ghia, U , Ghia, K N , and Shin, C T , 1982, High-Re Solution for Incompressible Flow Using the Navier-Stokes Equations and a Multigrid Method, J of Comput Phys., vol 48, pp 387 - 411.

[9] Gresho, P M. and Sani, R. L , 1987, International J. of Numerical Methods in Fluids, vol 7, pp 1111

[10] Harlow, F H and Welch, J E , 1965, Numerical Calculation of Time-Dependent Viscous Incompressible Flow of Fluids with Free Surfaces, Physics of Fluids, vol. 8, pp 2182-2189

[11] Hao, Y L and Tao, Y., X , 1999, A Continua Model for Three- Dimensional Convective Melting of Solid Particles in A Fluid under Micro-Gravity, Preprint

[12] Harten, A , 1983, High Resolution Schemes for Hyperbolic Conservation Laws, J of Comput. Phys , vol 49, 357-393.

[13] Hirt, C W , and Nichols, B D , Volume of Fluid (VOF) Method for the Dynamics of Free Boundaries, J Comput Phys , vol 39, pp. 201-225

[14] Kim, J and Moin, P. , 1985, Application of a Fractional-Step Method to Incompressible Navier-Stokes Equations, J of Comput. Phys , vol 59, pp 308 - 323

[15] Ladyzhenskaya, O., A., 1969, The Mathematical Theory of Viscous Incompressible Flow, 2nd edition, Gordon and Beach, New York

[16] MacCormack, R. W. , 1985, Current Status of Numerical Solutions of the Navier-Stokes Equations, American Institute of Aeronautics and Astronautics Paper 85-0032.

[17] Roe, P L , 1981, Approximate Riemann Solvers, Parameter Vectors, and Difference Schemes, J. of Compt Phys , vol 43, pp 357-372

[18] Schlichting, H., 1979, Boundary Layer Theory, 7th edition, McGraw-Hill, New York

[19] Shen, J, and Temam, R, 1989, A New Fractional Scheme for the Approximation of Incompressible Flows, Math Appli Comp vol. 8, pp 3-22

[20] Temam, R , 1979, Navier-Stokes Equations, Theory and Numerical Analysis, 2nd edition, North-Holland, Amsterdam

[21] Temam, R., 1995, Navier-Stokes Equations and Nonlinear Functional Analysis, 2nd edition, SIAM CBMS-NSF regional conference series in applied mathematics, Philadelphia

[22] Van Kan, J 1986, A Second-Order Accurate Pressure Correction Scheme for Viscous Incompressible FLow, SIAM J Sci. Stat. Comput., vol 7, No 3, pp 870- 891.

[23] Williams, P. T., 1993, Continuity Constraint Method A Finite Element Computational Fluid Dynamics Algorithm for Incompressible Navier-Stokes Fluid Flows, PhD Dissertation, UT-Knoxville.

[24] Wong, K L., 1995, A Parallel Finite Element Algorithm for 3D Incompressible Flow in Velocity-Vorticity form, PhD Dissertation, UT-Knoxville

[25] Yanenko, N. N , 1971, The Method of Fractional Steps, Springer-Verlag, New York

Vita

Mr. Bo Chen was born in July 2, 1969 in Beijing, People's Republic of China He attended the primary school in 1977 In July 1982, he was admitted to No 8 middle school of Beijing and then he spent 6 years there for his secondary education. In September 1992, he entered the Beijing Institute of Aeronautics and Astronautics as an undergraduate student He got his Bachelor of Engineering degree in July, 1992 Then he was employed as a junior research staff in the Institute of Engineering Thermo-physics, Chinese Academy of Sciences At the end of 1995, he went to England to have his postgraduate study at the University of Durham In July 1997 he passed the final exam and got his MSc degree in engineering. In August 1997, he came to the United States and attended the University of Tennessee, Knoxville where he changed to study mathematics. He will obtain his MSc degree in mathematics in December, 2000